EGE UNIVERSITY
GRADUATE SCHOOL
OF NATURAL AND APPLIED SCIENCES

(DOCTOR OF PHYLOSOPHY THESIS)

SYNTHESIS OF POLYMER-CLAY NANOCOMPOSITE

Ayhan ORAL
Department of Chemistry
Code of disciplin:405.04.01 (Physical Chemistry)
Date of presentation:17-09-2007

Supervisor: **Çetin GÜLER,Ph.D.**
Professor of Physical Chemistry
Assoc. Prof. Dr. Talal SHAHWAN
Ph.D. Professor of Physical Chemistry

Bornova, IZMIR (TURKEY)
2007

II

Ayhan ORAL tarafından doktora tezi olarak sunulan **"*Polimer-kil Nanokompozitinin Sentezi* "** başlıklı bu çalışma E. Ü. Lisansüstü Eğitim ve Öğretim Yönetmeliği ile E. Ü. Fen Bilimleri Enstitüsü Eğitim ve Öğretim Yönergesi'nin ilgili hükümleri uyarınca tarafımızdan değerlendirilerek savunmaya değer bulunmuş ve **17–09–2007** tarihinde yapılan tez savunma sınavında aday oybirliği / oyçokluğu ile başarılı bulunmuştur.

Jüri Üyeleri:	İmza
Jüri Başkanı :……..	……...
Raportör Üye : …….	…….....
Üye : …….	……
Üye : …….	…….....
Üye : …….	……

ÖZET

POLİMER-KİL NANOKOMPOZİTİNİN SENTEZİ

ORAL, Ayhan

Doktora Tezi, Kimya Anabilim Dalı
Danışman: Çetin GÜLER,
Doç. Dr. Talal SHAHWAN
Eylül, 2007, 108 Sayfa

Bu tezin amacı; hem katyon, hem de ATRP başlatıcı ucu olan iki fonksiyonlu bir başlatıcı sentezlemek ve bu başlatıcı ile geliştirilmiş özelliklere sahip nanokompozit elde etmektir. Başlatıcının içerdiği fonksiyonel guruplardan biri kuaterner amonyum tuzu ve diğeri ATRP başlatıcısı olan alkil halojenürdür. Bu başlatıcı ile hem montmorillonitin modifikasyonu hem de polimerleşme reaksiyonu gerçekleştirilecektir.

ATRP başlatıcısı montmorillonitin tabakalar arası boşluğuna sokuldu. Bu durumda polimeşme tabakalar arasında yürütüldü, polimer zincirleri arttı, bu kil tabakalarını dağıtmaya başladı, tabakaları açılmış ve dağılmış nanokompozite neden oldu.

HEMA/kil nanokompoziti; *yerinde (insitu)* polimerleşme yöntemiyle, kil partiküllerinin silikat galerilerine tutturulan başlatıcı ile sentezlendi. Polimerleşme reaksiyonu (methyl ethyl ketone ve 1-propanol) çözücü karışımında, 55^0C'de, önceden sentezlenmiş olan başlatıcı ile CuBr katalizörlüğünde ve 2, 2'-bipyridyl ligandı eşliğinde gerçekleştirildi. Tüm ürünler FT-IR, ^{1}H-NMR, ^{13}C-NMR, TEM, ve XRD yardımıyla karekterize edildi. Tg ve bozunma sıcaklığı gibi bazı termal parametreler TGA ve DSC aracılığı ile incelendi.

Anahtar sözcükler: Montmorillonit, HEMA, ATRP, Nanokompozit.

ABSTRACT

SYNTHESIS OF POLYMER-CLAY NANOCOMPOSITE

ORAL, Ayhan

Department of Chemistry

Supervisor: Çetin GÜLER,
Ph.D. Professor of Physical Chemistry
Assoc. Prof. Dr. Talal SHAHWAN
Ph.D. Professor of Physical Chemistry

September, 2007, 108 Pages

The objectives of this thesis are to develop a difunctional modificator; which has both cation and ATRP-initiator moiety and to synthesis nanocomposite with improved physical properties. In order to achieve these, difunctional initiator were designed and synthesized. The modificator consists of two parts; first part is a quaternary ammonium salt moiety and second is an ATRP-initiator moiety. Synthesized

materials have both cation and ATRP-initiator moiety. Namely, it will modify both montmorillonite and initiate the polymerization.

ATRP initiator was intercalated into the interlayer spacings of the montmorillonite. In this situation the polymerization inside the galleries progresses and the polymer chain density increases, the layers will be pushed gradually apart and eventually delaminate, leading to a well-dispersed and intercalated nanocomposite.

The HEMA/clay nanocomposite was synthesized by in situ Atom Transfer Radical Polymerization (ATRP) from initiator moieties immobilized within the silicate galleries of the clay particles. Polymerization reaction was carried out in a mixed solvent system consisting of methyl ethyl ketone and 1-propanol at 55 °C, used the initiator that has been already synthesized with a copper bromide catalyst. The 2, 2'-bipyridyl (bpy) complex was used as ligand.

All of the products were characterized via FT-IR, ^{1}H-NMR, ^{13}C-NMR, TEM, and XRD. Some thermal parameters such as Tg and degradation temperature were investigated via TGA and DSC.

Keywords: Montmorillonite, HEMA, ATRP, Nanocomposite.

ACKNOWLEDGMENT

I would like to thank to Professor Çetin GÜLER for his supervising and kind assistance throughout this study. I would also like to thank to Associate Professor Talal SHAHWAN of Department of Chemistry of İYTE for his contribution of the thesis and some instrumental analyses. I would also like to thank to Professor Turgay SEÇKİN of Department of Chemistry of Inönü University for his contribution of the thesis and some instrumental analyses.

I am also grateful to Mahmut ULUSOY and Kadir AY of a research assistant of the Department of Chemistry. I would also like to thank to Özge TUNUSOĞLU of Department of Chemistry of İYTE for her contribution of the thesis and some instrumental analyses.

My special thanks are extended to my dear family for their support and encouragement.

19-07-2007 Ayhan ORAL

CONTENTS

Page

CONTENTS (Continued)

Page

CONTENTS (Continued)

Page

LIST OF FIGURES

Figure **Page**

LIST OF FIGURES (Continued)

Figure **Page**

LIST OF FIGURES (Continued)

Figure **Page**

LIST OF FIGURES (Continued)

Figure **Page**

LIST OF TABLES

ABBREVIATIONS

Abbreviations		Explanation
ATRP	:	Atom Transfer Radical Polymerization
HEMA	:	Hydroxyethyl Methacrylate
Bpy	:	2, 2'-Bipyridyl
NMR	:	Nuclear Magnetic Resonance
TEM	:	Transmission Electronic Spectroscopy
XRD	:	X-ray Diffraction
Tg	:	Glass Transition Temperature
TGA	:	Thermogravimetric Analysis
DSC	:	Differential Scanning Calorimetry
PLS	:	Polymer/layered Silicate
PCN	:	Polymer-clay Nanocomposites
MMT	:	Montmorillonite
CEC	:	Cation Exchange Capacity
PVA	:	Poly(vinyl alcohol)
PEO	:	Poly(ethylene oxide)
FTIR	:	Fourier Transform Infrared
LFRP	:	Lliving Free Radical Polymerizations
OMLS	:	Organically Modified Layered Silicates
CRP	:	Controlled Living Radical Polymerization
PDI	:	Polymer Distrubution Index
ATRA	:	Atom Transfer Radical Addition
k_{act}	:	Rate Constant of Activation
k_{deact}	:	Rate Constant of Deactivation

ABBREVIATIONS (Continued)

***k*p**	:	Rate Constant of Propagation
k_t	:	Termination reactions
K_{eq}	:	Equilibrium Constant
DP	:	Degree of Polymerisation
MMA	:	Methyl Methacrylate
M_w	:	Viscosity Average Molecular Weight
M_n	:	Number Average Molecular Weight
K	:	Equilibrium Constants
OSET	:	Outer-sphere Electron Transfer
pMMA	:	Poly- Methyl Methacrylate
GPC	:	Gel Permeation Chromatography
BzO_2	:	Benzoyl Peroxide
WAXD	:	Wide Angle X-ray Diffraction
MWD	:	Molecular Weight Distribution
MEK	:	Methyl ethyl ketone
Bpy	:	2, 2'-Bipyridine
DCM	:	Dichloromethane
R-X	:	Alkylammonium Initiator
$M^n X^n L$	:	Metal Complex
R^*	:	Radical Species
DMF	:	*N,N*-Dimethylformamide
CBZ	:	Benzyl Chloroformate
TFA	:	Trifluoroacetic Acid
BOC	:	di-tert-butyldicarbonate
CTAB	:	Cetyltrimethylammonium Bromide

1. INTRODUCTION

The vulcanization of natural rubber and synthesis of the polymeric materials has appeared as a new class in chemistry that is called polymer chemistry. Polymers had been synthesized and used in the 19th century and are still among the important materials for industry today. Polymer chemistry provides a lot of tools for people but more tools are required for using in various purpose. New tools required new materials that have various physical and chemical properties. For this requirement, Polymer Technology has evolved from simple polymers to composite-materials. Manufacturers and scientists fill polymers with particles in order to improve the physical, thermal and chemical properties of the polymers and to reduce cost.

Nanocomposites are a new class of composites that are particle-filled polymers for which at least one dimension of the dispersed particles is in the nanometer range. Clays are very cheap, therefore used as filler in polymers, but no reinforcing effect, since no homogeneous molecular distribution within the matrix. For the best distribution in the polymer matrix, clays are modified and so layered silicate is formed.

In recent year's polymer/layered silicate (PLS) nanocomposites have attracted strong interest, both in industry and in academia, because of the combination of both the properties of the inorganic nano particles and those of the polymer. Nanocomposites often exhibit remarkable improvement in materials properties when compared with virgin polymer or conventional micro and macro-composites. These improvements can

include high moduli [Okada et al.,1990; Giannelis, 1996 ; Giannelis et al., 1999; Le Baron et al., 1999; Vaia et al., 1999; Biswas and Ray, 2001;], increased strength and heat resistance [Giannelis, 1998], decreased gas permeability [Xu et al.,2001; Bharadwaj, 1989; Messersmith et al., 1995; [a]Yano et al.,1993; Kojima et al.,1993;] and flammability [Gilman et al., 1997; Gilman, 1999; Dabrowski et al., 1999; Bourbigot et al.,2000; Gilman et al., 2000], and increased biodegradability of biodegradable polymers [Ray et al., 2002]. The field of PLS nanocomposites has gained momentum recently because of these properties and very small amounts of layered silicate loadings resulted in pronounced improvements. For these reasons "Nanocomposites" are most important materials in industry and chemistry.

Several strategies have been considered to prepare PCNs, including the four main processes of exfoliation adsorption, in situ intercalative polymerization, solution intercalation and melt intercalation.

This thesis is concerned with using Montmorillonite for synthesis of nanocomposite via ATRP. Resulting materials have improving properties. This work is divided into two parts, the first part dealing with the synthesis and characterization of difunctional modification cation. The second parts deals with the synthesis and characterization of nanocomposite.

The monomer chosen was hydroxyethyl methacrylate (HEMA) for the nanocomposite. Montmorillonite was preferred as a filler and

inorganic component of the nanocomposite. Atom transfer radical polymerization (ATRP) was the method chosen to synthesize our nanocomposite.

1.1. Structure and Properties of Layered Silicates

The layered silicates commonly used in of PLS nanocomposites belong to the same general family of 2:1 layered or phyllosilicates. Their crystal lattice consists of two-dimensional layers where a central octahedral sheet of alumina or magnesia is fused to two external silica tetrahedron by the tip so that the oxygen ions of the octahedral sheet do also belong to the tetrahedral sheets. The layer thickness is around 1 nm, and the lateral dimensions of these layers may vary from 30 nm to several microns or larger, depending on the particular silicate. These layers organize themselves to form stacks with a regular van der Walls gap in between them called the interlayer or the gallery. Isomorphic substitution within the layers (for example, Al^{3+} replaced by Mg^{2+} or Fe^{2+}, or Mg^{2+} replaced by Li^{1+}) generates negative charges that are counterbalanced by alkali and alkaline earth cations situated in the interlayer. As the forces that hold the stacks together are relatively weak, the intercalation of small molecules between the layers is easy [Bourbigot et al., 2000]. In order to render these hydrophilic phyllosilicates more organophilic, the hydrated cations of the interlayer can be exchanged with cationic surfactants such as alkylammonium or alkylphosphonium (onium). The modified clay (or organoclay) being organophilic, its surface energy is lowered and is more compatible with

organic polymers. These polymers may be able to intercalate within the galleries, under well defined experimental conditions.

MMT, hectorite, and saponite are the most commonly used layered silicates. Layered silicates have two types of structure: tetrahedral-substituted and octahedral substituted. In the case of tetrahedrally substituted layered silicates the negative charge is located on the surface of silicate layers, and hence, the polymer matrices can react interact more readily with these than with octahedrally-substituted material. Details regarding the structure and chemistry for these layered silicates are provided in figure 1.1 and table 1.1.

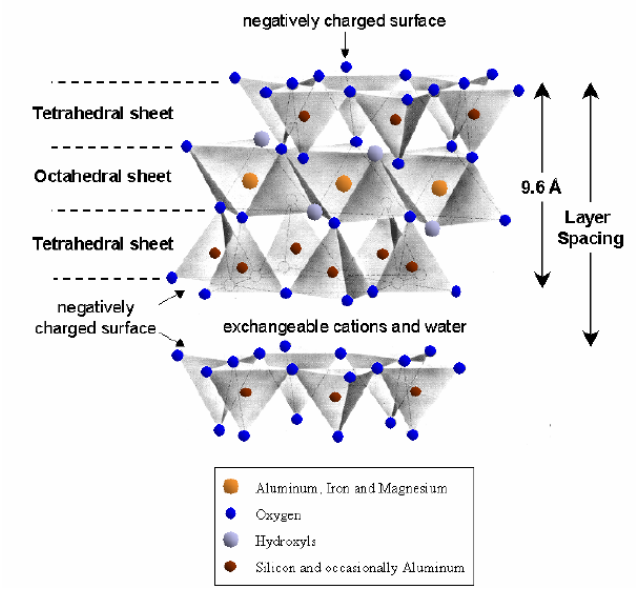

Figure 1.1. The Structure of Montmorillonite

Table 1.1 Chemical formula and characteristic parameter of commonly used 2:1 phyllosilicates

Table 1
Chemical formula and characteristic parameter of commonly used 2:1 phyllosilicates

2:1 phyllosilicates	Chemical formula	CEC (mequiv/100 g)	Particle length (nm)
Montmorillonite	$Mx(Al_{4-x}Mg_x)Si_8O_{20}(OH)_4$	110	100–150
Hectorite	$Mx(Mg_{6-x}Li_x)Si_8O_{20}(OH)_4$	120	200–300
Saponite	$MxMg_6(Si_{8-x}Al_x)Si_8O_{20}(OH)_4$	86.6	50–60

M, monovalent cation; *x*, degree of isomorphous substitution (between 0.5 and 1.3).

These types of layered silicates are characterized by a moderate surface charge known as the cation exchange capacity (CEC), and generally expressed as mequiv/100 g. This charge is not locally constant, but varies from layer to layer, and must be considered as an average value over the whole crystal. Even if small parts of the charge balancing cations are located on the external crystallite surface, the majority of these exchangeable cations are located inside the galleries.

Layered silicates have two particular characteristics, which are generally considered for PLS nanocomposites. The first is the ability of the silicate particles to disperse into individual layers. The second characteristic is the ability to fine-tune their surface chemistry through ion exchange reactions with organic and inorganic cations. These two characteristics are, of course, interrelated since the degree of dispersion of layered silicate in a particular polymer matrix depends on the interlayer cation.

1.2. Structure and Properties of Nanocomposites

The physical mixture of a polymer and layered silicate may not form a nanocomposite. This situation is analogous to polymer composites, and in most cases separation into discrete phases takes place. In immiscible systems, which typically correspond to the more conventionally filled polymers, the poor physical interaction between the organic and the inorganic components leads to poor mechanical, thermal properties and agglomeration in polymer matrix. In contrast, strong interactions between the polymer and the layered silicate in PLS nanocomposites lead to the organic and inorganic phases being dispersed at the nanometer level. As a result, nanocomposites exhibit unique properties not shared by their micro counterparts or conventionally filled polymers moduli [Okada et al.,1990; Giannelis, 1996; Giannelis et al., 1999; Le Baron et al., 1999; Vaia and Giannelis, 1999 ; Biswas and Ray, 2001].

Pristine layered silicates usually contain hydrated Na^+ or K^+ ions [Brindly et al., 1980]. Obviously, in this pristine state, layered silicates are only miscible with hydrophilic polymers, such as poly(ethylene oxide) (PEO) [Aranda and Hitzky, 1992], or poly(vinyl alcohol) (PVA) [Greenland, 1963]. To render layered silicates miscible with other polymer matrices, one must convert the normally hydrophilic silicate surface to an organophilic one, making the intercalation of many engineering polymers possible. Generally, this can be done by ion-exchange reactions with cationic surfactants including primary,

secondary, tertiary, and quaternary alkylammonium or alkylphosphonium cations. Alkylammonium or alkylphosphonium cations in the organosilicates lower the surface energy of the inorganic host and improve the wetting characteristics of the polymer matrix, and result in a larger interlayer spacing. Additionally, the alkylammonium or alkylphosphonium cations can provide functional groups that can react with the polymer matrix, or in some cases initiate the polymerization of monomers to improve the strength of the interface between the inorganic and the polymer matrix(Blumstein, 1965; Krishnamoorti and Giannelis, 1996).

In order to describe the structure of the interlayer in organoclays, determine the orientation and arrangement of the alkyl chain was performed using X-ray diffraction (XRD). Depending on the packing density, temperature and alkyl chain length, the chains were thought to lie either parallel to the silicate layers forming mono or bilayers, or radiate away from the silicate layers forming mono or bimolecular arrangements figure 1.2 (Lagaly, 1986). However, these idealized structures have been shown to be unrealistic by Vaia et al. (Vaia et al., 1994) using FTIR experiments. By monitoring frequency shifts of the asymmetric CH_2 stretching and bending vibrations, they found that the intercalated chains exist in states with varying degrees of order. In general, as the interlayer packing density or the chain length decreases (or the temperature increases), the intercalated chains adopt a more disordered, liquid-like structure resulting from an increase in the gauche/trans conformer ratio figure 1.3. When the available surface

area per molecule is within a certain range, the chains are not completely disordered but retain some orientational order similar to that in the liquid crystalline state.

This interpretation has been recently confirmed by molecular dynamics simulations where a strong layering behavior with a disordered liquid-like arrangement has been found, that can evolve towards a more ordered arrangement by increasing the chain length [Hackett et al., 1998]. As the chain length increases, the interlayer structure appears to evolve in a stepwise fashion, from a disordered to more ordered monolayer then `jumping' to a more disordered pseudo-bilayer.

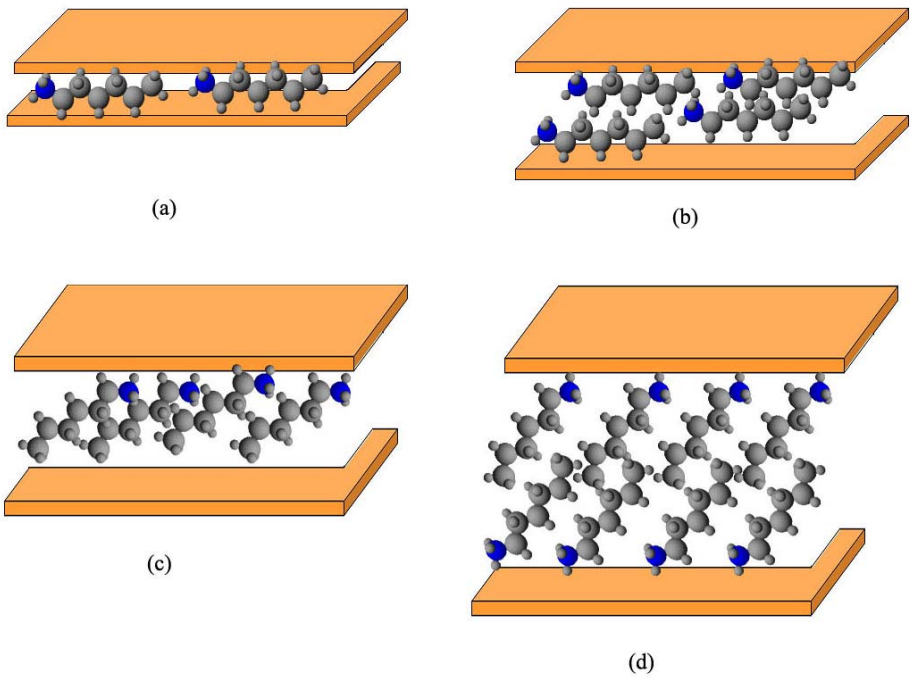

Figure 1.2. Alkyl Chain Aggregation In Layered Silicates: (a) lateral monolayer; (b) lateral bilayer; (c) paraffin-type monolayer and (d) paraffin-type bilayer

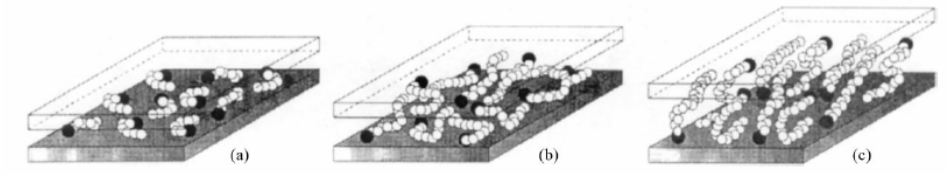

Figure 1.3. Alkyl Chain Aggregation Models: (A) Short Chain Lengths, The Molecules Are Effectively Isolated From Each Other, (B) Medium Lengths, Quasi-Discrete Layers Form With Various Degree Of In Plane Disorder And Interdigitation Between The Layers And (C) Long Lengths, Interlayer Order Increases Leading To A Liquid-Crystalline Polymer Environment. Open Circles Represent The CH_2 Segments While Cationic Head Groups Are Represented By Filled Circles [Vaia et al., 1994].

1.3. Types of Nanocomposites

In general, layered silicates have layer thickness on the order of 1 nm and a very high aspect ratio (e.g. 10–1000). A few weight percent of layered silicates that are properly dispersed throughout the polymer matrix thus create much higher surface area for polymer/filler interaction as compared to conventional composites. Depending on the strength of interfacial interactions between the polymer matrix and layered silicate (modified or not), three different types of PLS nanocomposites are thermodynamically achievable figure 1.4:

a. Intercalated nanocomposites: in intercalated nanocomposites, the insertion of a polymer matrix into the layered silicate structure occurs in a crystallographically regular fashion, regardless of the clay to polymer ratio. Intercalated nanocomposites are normally interlayer by a

few molecular layers of polymer. Properties of the composites typically resemble those of ceramic materials.

b. Flocculated nanocomposites: conceptually this is same as intercalated nanocomposites. However, silicate layers are some times flocculated due to hydroxylated edge–edge interaction of the silicate layers.

c. Exfoliated nanocomposites: in an exfoliated nanocomposite, the individual clay layers are separated in a continuous polymer matrix by an average distances that depends on clay loading. Usually, the clay content of an exfoliated nanocomposite is much lower than that of an intercalated nanocomposite.

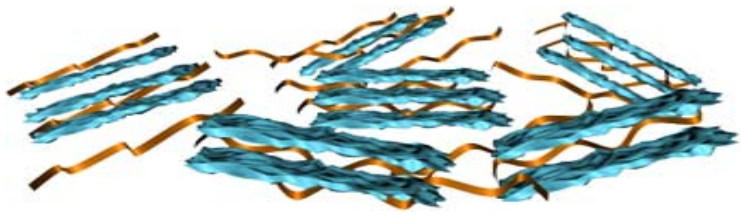

a) Intercalated

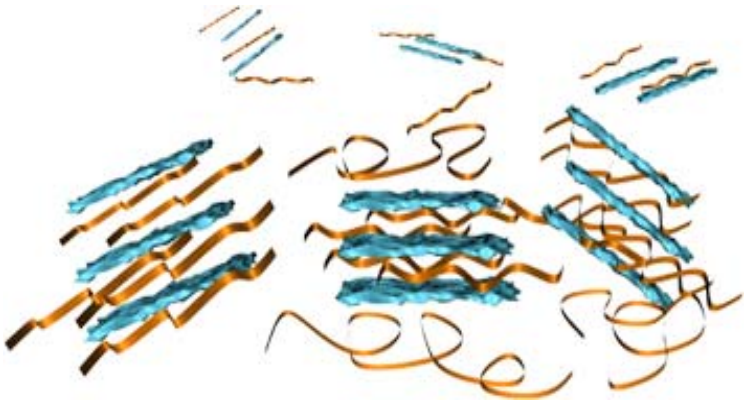

b) Intercalated and Flocculated

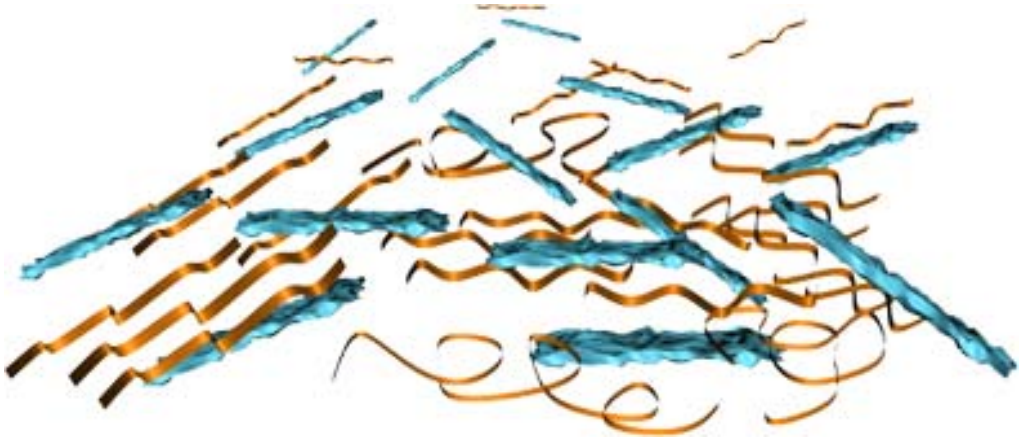

a) Exfoliated

Figure 1.4. Schematically Illustration Of Three Different Types Of Thermodynamically Achievable Polymer/Layered Silicate Nanocomposites ([a]Ray et al., 2003).

2. NANOCOMPOSITE PREPERATION

2.1. Modification of the Clays

Normally, when organic and inorganic materials are mixed with each other, interactions between organic and inorganic materials may not have a strong. Namely, inorganic particles can not be dispersed in polymer matrix. For that reason, to achieve of best dispersion compatibilizing agents are used. The compatibilizing agents used in the synthesis of nanocomposites (polyamide 6-clay hybrids) were amino acids (Okada et al., 1990), alkylammonium ions, phosphonium ions, silanes, aminomethylstyrene (Laus et al., 1998) and living free radical

polymerizations initiator (LFRP) (Weimer et al., 1999). Modification process based on cation exchange basis. The cation-exchange process is occurred between alkylammonium ions and cations initially intercalated between the clay layers.

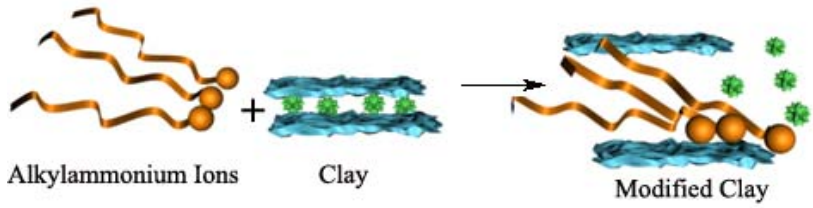

Figure 2.1. The Cation-Exchange Process (Spheres Represent NH3+ And Stars Represent Exchangeable Cations).

Polymer intercalation or exfoliation depends on silicate functionalization and constituent interactions. An optimal interlayer structure on the OMLS, with respect to the number per unit area and size of surfactant chains, is most favorable for nanocomposite formation, and (b) polymer intercalation depends on the existence of polar interactions between the OMLS and the polymer matrix.

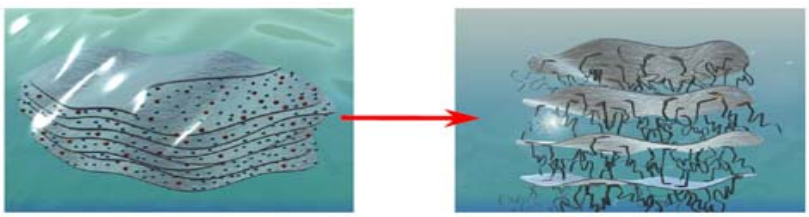

Figure 2.2. The Cation-Exchange Representation (Okada Et Al., 1990)
A) C^{+n}mmt B) Alkylammonium Ions Exchanged MMT (modified MMT)

Polymer-layered silicate nanocomposites have been prepared various methods. They include four main processes [Oriakhi et al., 1998].

2.1.1. Template Synthesis

This technique, where the silicates are formed in situ in an aqueous solution containing the polymer and the silicate building blocks has been widely used for the synthesis of double-layer hydroxide-based nanocomposites [Wilson Jr et al., 1999; Oriakhi et al., 1997] but is far less developed for layered silicates. In this technique, based on self-assembly forces, the polymer aids the nucleation and growth of the inorganic host crystals and gets trapped within the layers as they grow. The following sections review the four aforementioned preparation techniques that will be illustrated with representative examples.

2.2. Exfoliation-adsorption

First, the layered silicate is swollen in the solvent. Then, the polymer, dissolved in the solvent, is added to the solution and intercalates between the clay layers. The last step consists in removing the solvent by evaporation usually under vacuum. figure 2.3 shows how the polymer is intercalated between the clay layers. Nanocomposites based on high-density polyethylene (Jeon et al., 1998), polyimide ([b]Yano et al., 1993), and nematic liquid crystal polymers (Kawasumi et al., 1998) have been synthesized by this method.

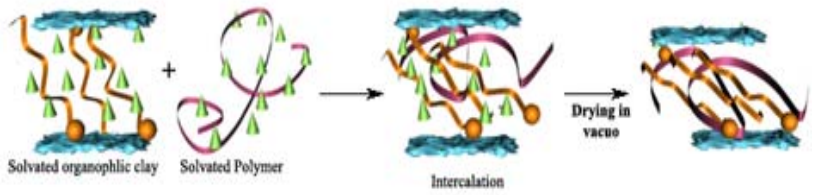

Figure 2.3. The Intercalation Of The Polymer By The "Solution" Approach (Green Cones Are Represent Solvent Molecules And Red Curve Represents Polymer Backbone).

The black dots represent the solvent molecules. If polymeric aqueous solutions are added to dispersions of fully delaminated sodium layered silicates, the strong interactions existing between the hydrosoluble macromolecules and the silicate layers often trigger the reaggregation of the layers. In this situation, the layers remain in colloidal distribution [Ogata et al., 1997].

For the overall process, in which polymer is exchanged with the previously intercalated solvent in the gallery, a negative variation in the Gibbs free energy is required. The driving force for the polymer intercalation into layered silicate from solution is the entropy gained by desorption of solvent molecules, which compensates for the decreased entropy of the confined, intercalated chains [Vaia and Giannelis, 1997]. Using this method, intercalation only occurs for certain polymer/solvent pairs. This method is good for the intercalation of polymers with little or no polarity into layered structures, and facilitates production of thin films with polymer-oriented clay intercalated layers. However, from commercial point of view, this method involves the copious use of

organic solvents, which is usually environmentally unfriendly and economically prohibitive.

If some polymeric materials such as poly (imides) or some conjugated polymers are not fusible and soluble in organic solvents, soluble polymeric precursors that can be intercalated in the layered silicate have been used. This has been successfully achieved by using the exfoliation-adsorption process.

In polymers water insoluble state; emulsion polymerization has been also studied in order to promote the intercalation of waterinsoluble polymers within Na-montmorillonite that is well known to readily delaminate in water [Lee and Jang, 1996; Lee and Jang, 1998]. Monomer was dispersed in the aqueous phase with the aid of a surfactant. Monomers are attracted onto and/or inside the layered silicates.

2.3. In Situ Intercalative Polymerization

First, the layered silicate is swollen in the monomer. This swelling process is related to mixing time, polarity of the monomer molecules, the surface treatment of the layered silicates, and temperature. Clay which has the high surface energy attracts polar monomer. Monomer can diffuse between the clay layers. When equilibrium is reached the diffusion stops and the clay has been swollen in the monomer to a certain extent corresponding to a perpendicular orientation of the alkyl ammonium ions (Messersmith et al., 1994). Polar monomers are easily

driven between the clay layers than less polar monomers. As this mechanism occurs, the organic molecules can eventually delaminate the clay. After the swelling initiator is added, then the polymerization reaction is initiated by an increase of temperature or radiation (Messersmith et al., 1995).

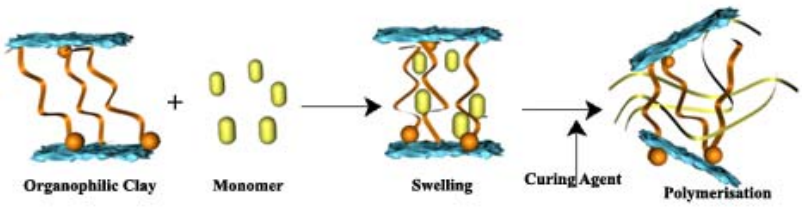

Figure 2.4. The "In-Situ Polymerization". Polar Monomer Molecules Diffuse Between The Layers.

The alkylammonium ions adopt a perpendicular orientation in order to optimize solvation interactions with the monomer. The polymerization reaction leads to the delamination of the clay.

2.4. Melt Intercalation

In this method, only thermoplastic polymers are used because of the preparation method. The layered silicate is mixed with polymer via extrusion and injection molding. The mixture is then annealed at a temperature above the glass transition temperature (Tg) of the polymer and forms a nanocomposite.

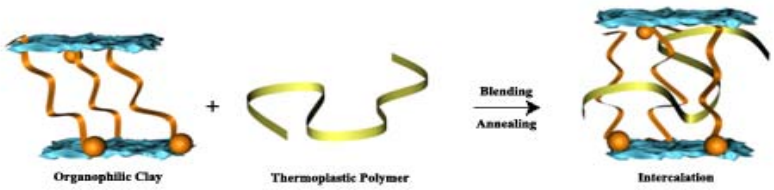

Figure 2.5. The "Melt Intercalation" Process.

As shown in Figure 2.5, the polymer chains dramatic loss of conformational entropy during the intercalation. The proposed driving force for this mechanism is the important enthalpic contribution of the polymer/organoclay interactions during the blending and annealing steps. The polymer chains loose conformational entropy as they get intercalated between the clay layers. The loss of conformational entropy of the polymer chains during the intercalation is possibly compensated by enthalpic interactions between the clay and the polymer.

The melt intercalation process has become increasingly popular because of its great potential for application in industry economically and easiness of process. This process has no organic solvent. For that reason it is environmentally.

3. TYPES OF POLYMERS

The large variety of polymer systems used in nanocomposites preparation with layered silicate can be conventionally given as below.

These include the vinylic polymers, condensation (step) polymers (N6, several polyamides, poly(1-caprolactone), poly(ethylene

terephthalate), poly(trimethylene terephthalate), poly(butylene terephthalate), polycarbonate, ethylene oxide copolymers, poly(ethylene imine), poly(dimethyl siloxane)…), polyolefins (polypropylene, polyethylene, polyethylene oligomers…), specialty polymers (N-heterocyclic polymers like polypyrrole, poly(N-vinylcarbazole), poly(p-phenylene vinylene)…), biodegradable polymers (polylactide, poly(butylene succinate), polyhydroxy butyrate…).

The monomers chosen were hydroxyethyl methacrylate (HEMA) as main component of the nanocomposite. HEMA is best known as the material used to make soft contact lenses, and has other applications in biomedical surface coatings, wound dressings, and drug delivery systems (Robbins E. M., 2002).

pHEMA was nominated as a viable candidate due to its high water content, bio-inert character, and resistance to hydrolysis, as well as its mechanical and optical properties. pHEMA has enjoyed widespread use as biomaterial hydrogel since the seminal work of Wichterle and Lim, and a variety of its properties have been studied and adjusted through copolymerization with other monomers (Montheard et al., 1992). Beyond its use in ophthalmic lenses (Wichterle et al., 1960; Khan and Percival, 1999), pHEMA has found application in drug delivery vehicles (Menapace et al., 1989; Seki et al., 1989), neural tissue templating (Sefton et al., 1980; Dalton et al., 2002), and hemocompatible films (Flynn et al., 2003; Ito et al., 1998; Terada et al., 1997; Nojiri et al., 1992). For example, copolymers of HEMA/styrene and HEMA/dimethyl

siloxane showed suppressed platelet adhesion and aggregation, and thus reduced thrombus formation (Terada et al., 1997).

4. ATOM TRANSFER RADICAL POLYMERIZATION (ATRP)

The living polymerization technique has expanded to include all chain-growth polymerization methods: cationic, anionic, transition metal-catalyzed, free radical polymerization. An ideal living polymerization is a chain-growth polymerization in which irreversible chain termination and chain transfer are absent. Therefore, once a chain is initiated, it will grow until no monomer is left. Unless a terminating agent is introduced, the living chain will remain active, so block copolymers can be synthesized via sequential addition of different monomers. Provided that the initiation efficiency is 100% and exchange between species of various reactivities is fast, the average molecular weight of the final polymer will be determined simply by the initial monomer/initiator ratio and the molecular weight distribution will be narrow. However, in practice, it is impossible to completely avoid chain transfer and chain termination reactions. Very often, the rates of these side reactions are controlled to be sufficiently slow such that well-defined polymers can be prepared. In such cases, the polymerizations are called “controlled/´living´ polymerizations” to indicate that, although chain transfer or chain termination may occur to some extent, the polymerizations are still as synthetically useful as the true living polymerization.

The synthesis of polymers with well-defined compositions, architectures, and functionalities has long been of great interest in polymer chemistry. The development of controlled/living radical polymerization (CRP) methods has been a long-standing goal in polymer chemistry, as a radical process is more tolerant of functional groups and impurities and is the leading industrial method to produce polymers (Matyjaszewski and Gaynor., 2000). The main difference between CRP and conventional radical polymerization (i.e., azobis (isobutyronitrile)/peroxide-initiated processes) is the lifetime of the propagating radical during the course of the reaction. In conventional radical processes, radicals generated by decomposition of initiator undergo propagation and bimolecular termination reactions are very fast (within a second). In contrast, the lifetime of a growing radical can be extended to several hours in a CRP. When the initiation is faster than, or at least comparable in rate to, propagation, the obtained polymers have narrow molecular weight distributions. These properties enable the preparation of polymers with predefined molecular weight, low polydispersity, controlled composition, and functionality.

Despite its tremendous industrial utility, CRP has not been realized until recently, largely due to the inevitable, near diffusion-controlled bimolecular radical coupling and disproportionation reactions. In CRP processes, the mechanism to extend the lifetime of growing radical utilizes a dynamic equilibration between dormant and active sites with rapid exchange between the two states. CRP requires the use of either persistent radical species or transfer agents to react with propagating

radicals to form the dormant species. Conversely, propagating radicals can be regenerated from the dormant species by an activation reaction.

One of the most versatile controlled radical polymerization techniques is atom transfer radical polymerization (ATRP) ([a]Matyjaszewski and Xia, 2001). In this method, polymers that have controlled molecular weight and PDI can be synthesized This method is based on establishing a rapid dynamic equilibration between a minute amount of growing free radicals and a large majority of the dormant species. The dormant chains may be alkyl halides, as in atom transfer radical polymerization (ATRP).

ATRP has its roots in atom transfer radical addition (ATRA), which targets the formation of 1:1 adducts of alkyl halides and alkenes, also catalyzed by transition metal complexes (Curran D. P., 1988). ATRA is a modification of Kharasch addition reaction figure 4.1 (Curran D. P., 1991). , which usually occurs in the presence of light or conventional radical initiators (Kharasch et al., 1945).

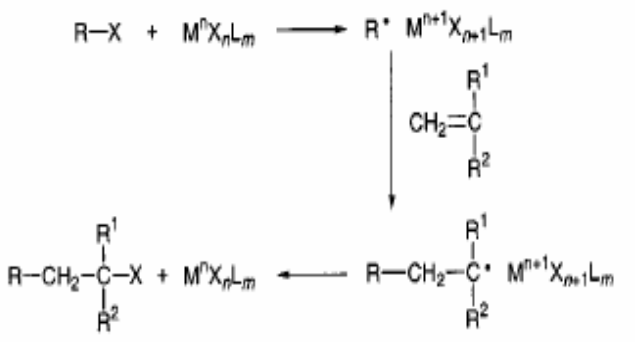

Figure 4.1. Metal-Catalyzed Radical Addition Reaction (Kharasch Addition Reaction)

Because of the involvement of transition metals in the activation and deactivation steps, chemo-, regio-, and stereoselectivities in ATRA and the Kharasch addition may be different. For example, under Kharasch conditions, in the reaction with chloroform the alkene will "insert" across the H-CCl_3 bond but in ATRA it will insert across the Cl-$CHCl_2$ bond, because the C-Cl bond is rapidly activated by the Fe(II) or Cu(I) complexes (Minisci et al., 1975). ATRP also has roots in the transition metal catalyzed telomerization reactions (Boutevin, 2000). These reactions, however, do not proceed with efficient exchange, which results in a nonlinear evolution of the molecular weights with conversions and polymers with high polydispersities. ATRP also has connections to the transition metal initiated redox processes as well as inhibition with transition metal compounds (Bamford et al., 1989; Bengough et al., 1971; Qiu and Matyjaszewski, 1997). These two techniques allow for either activation or deactivation process, however, without efficient reversibility. ATRP was developed by designing an appropriate catalyst (transition metal compound and ligands), using an initiator with the suitable structure, and adjusting the polymerization conditions such that the molecular weights increased linearly with conversion and the polydispersities were typical of a living process (Kato et al., 1995; [a]Wang and Matyjaszewski, 1995; Matyjaszewski et al.,; [b]Wang and Matyjaszewski, 1995; Percec and Barboiu, 1995). This allowed for an unprecedented control over the chain topology (stars, combs, branched), the composition (block, gradient, alternating, statistical), and the end functionality for a large range of radically polymerizable monomers ([p3]Matyjaszewski et al., [p1]Matyjaszewski et al.,

[p2]Matyjaszewski et al.; Patten and Matyjaszewski, 1998; Matyjaszewski, 1999; Patten and Matyjaszewski, 1999). Earlier attempts with heterogeneous catalyst and inefficient initiators were less successful (Otsu et al., 1990).

A general mechanism for ATRP is shown in figure 4.2. The radicals, or the active species, are generated through a reversible redox process catalyzed by a transition metal complex (M^n-Y/Ligand)

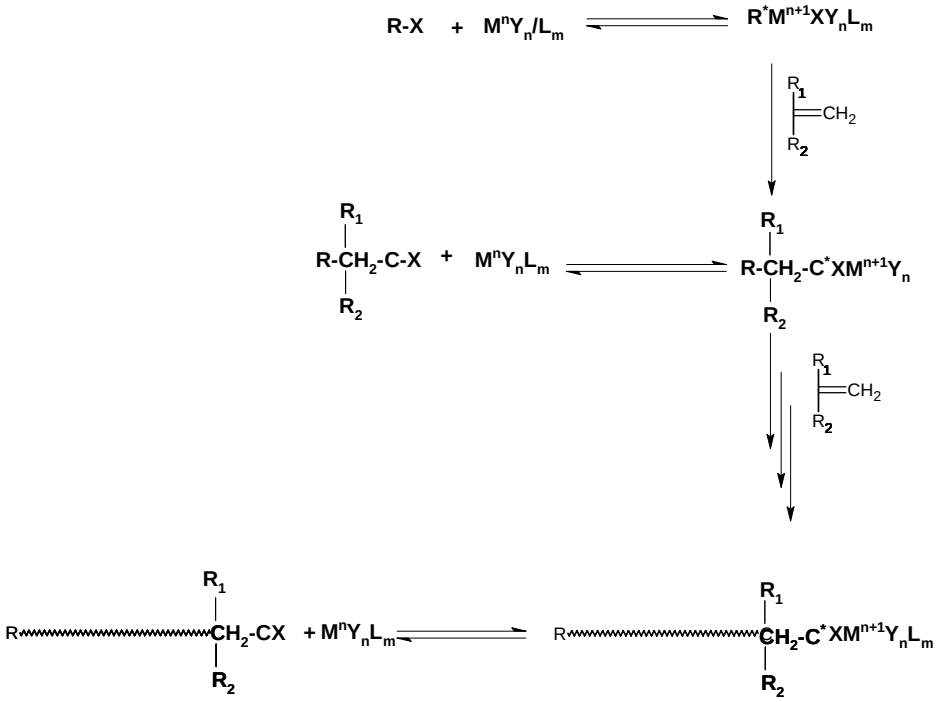

Figure 4.2. The Mechanism of ATRP.

A schematic representation of the mechanism of ATRP is displayed in Figure 4.2. ATRP consist of three parts. These parts are transition metal complex, initiating alkyl halides and ligand. $Mt^nY_mL_m$ is transition

metal complex, where Y may be another ligand or the counterion which undergoes a one electron oxidation with concomitant abstraction of a (pseudo) halogen atom, X, from a dormant species, R-X. The reaction is initiated by the activation (homolytic cleavage) of the carbon-halogen bond in an appropriate organic halide (R-X) via one-electron oxidation of the metal center (M^n X^nL) to form an initiating radical species (R^*) and an oxidized metal compound ($M^{n+1}XY_mL_m$). The R^* reacts with the halogen on the oxidized metal to regenerate R-X or adds to the monomer to generate a radial species [R-CH_2-$C(R_1)(R_2)^*$]. It is sooner or later transformed into the adduct [R-CH_2-$C(R_1)(R_2)$-X] of R-X and the monomer via abstraction of a halogen atom from ($M^{n+1}X^{n+1}L^m$). The carbon-halogen bond of adduct is subsequently activated by the metal complex, similarly to R-X, to result in a similar carbon-halogen bond at the polymer terminal via a repetitive set of the reactions. The key factors for these reactions are the low concentration of the radical intermediates at a given time and their fast but reversible transformation into the dormant species before undergoing successive addition to monomers. This process occurs with a rate constant of activation, k_{act}, and deactivation k_{deact}. Polymer chains grow by the addition of the intermediate radicals to monomers in a manner similar to a conventional radical polymerization, with the rate constant of propagation kp. Termination reactions (k_t) also occur in ATRP, mainly through radical coupling and disproportionation; however, in a well-controlled ATRP, no more than a few percent of the polymer chains undergo termination. Other side reactions may additionally limit the achievable molecular weights. Typically, no more than 5% of the total growing polymer chains

terminate during the initial, short, nonstationary stage of the polymerization. This process generates oxidized metal complexes, X-M^{n+1}, as persistent radicals to reduce the stationary concentration of growing radicals and thereby minimize the contribution of termination (Giannelis, 1998). A successful ATRP will have not only a small contribution of terminated chains, but also a uniform growth of all the chains, which is accomplished through fast initiation and rapid reversible deactivation.

ATRP is multicomponent system that composed of the monomer, an initiator (alkyl halogen which has transferable (pseudo) halogen, transition metal compound, suitable ligand and solvent. Sometimes an additive is used. For a successful ATRP, other factors, such as reaction time and temperature, must also be taken into consideration. All of these factors effect on ATRP will be investigated respectively.

4.1. ATRP Monomers

ATRP is the effective method to polymerise vinyl type monomers such as styrene ([d]Matyjaszewski et al., 1997; Qiu and Matyjaszewski, 1997; Percec and Barboiu, 1995), acrylates (Davis et al., 1999; [b]Matyjaszewski et al., 1997), methacrylates (Wang et al., 1997; Haddleton et al., 1997), acrylonitrile ([c]Matyjaszewski et al., 1997), (meth)acrylamides (Teodorescu and Matyjaszewski, 2000; [b]Matyjaszewski et al., 1998), dienes (Matyjaszewski et al.,). Very recently, living radical polymerizations of vinyl acetate (Wakioka et al.,

2002) and vinyl chloride (Percec et al., 2002) were investigated by Sawamoto and Percec.

Some monomers cannot be polymerized by this method. Such as; ethylene and α-olefins which are less reactive, acrylic and methacrylic acid monomers that would rather complexation with metal than polymerization.

Each monomer has its own unique atom transfer equilibrium constant for its active and dormant species. The polymerization rate is concerned with product of k_p and the equilibrium constant (K_{eq}) k_{act}/k_{deact}). ATRP will occur very slowly if the equilibrium constant is too small. For that reason less reactive monomers such as olefins, halogenated alkenes, and vinyl acetate has not yet been polymerized yet. Because each monomer has a specific equilibrium constant, optimal condition for polymerization which include concentration and type of the catalyst, temperature, solvent, and some additives may be quite different. If equilibrium constant is high enough, large amount of termination will occur because of a high radical concentration. This will be accompanied by a large amount of deactivating higher oxidation state metal complex; which will shift the equilibrium toward dormant species and may result in the apparently slower polymerization (Queffelec et al., 2000).

4.2. ATRP Initiators

The amount of the initiator in the ATRP determines the final molecular weight of the polymer at full monomer conversion according to formula as below.

$DP = \Delta[M] \ /[\mathrm{I}]_o$

First of all, for a effective ATRP initiating system two parameters are important. First, initiation step should be faster than propagation step. Second, the probability of side reactions should be minimized. Analogous to the "living" carbocationic systems, the main factors that determine the overall rate constants are the equilibrium constants rather than the absolute rate constants of addition (Matyjaszewski et al., 1996; Matyjaszewski and Sigwalt, 1994). There are several general considerations for the initiator choice. (1) The stabilizing group order in the initiator is roughly CN > C(O)R > C(O)OR > Ph >Cl > Me. Multiple functional groups may increase the activity of the alkyl halide, e.g., carbon tetrachloride, benzhydryl derivatives, and malonates. Tertiary alkyl halides are better initiators than secondary ones, which are better than primary alkyl halides. These have been partially confirmed by recent measurements of activation rate constants (Goto and Fukuda, 1999; [b]Matyjaszewski et al., 2001; [c]Matyjaszewski et al., 2001). Sulfonyl chlorides also provide faster initiation than propagation. (2) The general order of bond strength in the alkyl halides is R-Cl > R-Br > R-I. Thus, alkyl chlorides should be the least efficient initiators and alkyl iodides the most efficient (because of the difference in electronegativity). But the using of alkyl iodides is very difficult. Because they are light sensitive,

metal iodide complexes are not stable (e.g., CuI_2 is thermodynamically unstable and cannot be isolated), the R-I bond may possibly be cleaved heterolytically, and there are potential complications of the ATRP process by degenerative transfer (Tatemoto and Oka, 1984; Matyjaszewski et al., 1995). Bromine and chlorine are the most frequently used halogens by far others. In general, the same halogen is used in the initiator and the metal salt (e.g., Br/CuBr); however, the halogen exchange can sometimes be used to obtain better polymerization control ([d]Matyjaszewski et al., 1998). In a mixed halide initiating system, R-X/Mt-Y (X, Y) Br or Cl), the bulk of the polymer chains are terminated by chlorine due to the stronger alkyl-chloride bond. Thus, the rate of initiation is increased relative to propagation and ethyl 2-bromoisobutyrate/CuCl leads to a better controlled polymerization of MMA in comparison to using ethyl 2-bromoisobutyrate/CuBr ([d]Matyjaszewski et al., 1998). The halogen exchange method also enables the use of alkyl halides of apparently lower reactivities in the polymerization of monomers with apparently higher equilibrium constants. This is especially important for the formation of block copolymers (Shipp et al., 1998; Tong et al., 2000; Leclere et al., 1999; Moineau et al., 2000). Pseudohalogens (e.g., SCN) have also been used in ATRP (Davis et al., 1997; Singha and Klumperman, 2000). Initiation using benzyl thiocyanate is slow for both styrene and MA, and *M*n higher than the theoretical values are obtained. Better results are obtained when alkyl halides are used as the initiators and CuSCN as the catalyst. Similarly, transition metal dithiocarbamates have been employed in the presence of AIBN to induce controlled reverse ATRP of styrene

at 120 °C. (3) Choice of catalyst is important effect on ATRP. For example, 2-bromoisobutyrophenone initiates the controlled polymerization of MMA catalyzed by ruthenium or nickel complexes but has not been successfully used in the copper-mediated ATRP. This is ascribed to the reduction of the resulting electrophilic radical by the copper(I) species as the copper catalysts have lower redox potentials. (4) The various experimental procedures and addition of the chemicals are effect on the ATRP. For example, slow addition of the benzhydryl chloride initiator to the$CuCl(dNbpy)_2$-catalyzed ATRP of MMA generates a lower concentration of benzhydryl radicals and thus reduces the rate of termination between the radicals. The diethyl 2-bromomalonate/CuBr system initiates the ATRP of styrene, and the polymerization was well controlled when the catalyst was added slowly to the initiator/monomer solution. This avoided the potential reduction of the malonyl radical by the copper(I) species. It may also be surprising, but the heterogeneous catalytic systems may provide more efficient initiation than homogeneous ones when very reactive alkyl halide initiators are used, most likely due to slow dissolution of the catalyst and hence its lower instantaneous concentration. For example, CCl_4 is a good initiator for styrene and MMA with $CuBr(bpy)_3$ as the catalyst ([b]Wang and Matyjaszewski, 1995), but the same is not true using the $CuBr(dNbpy)_2$ catalytic system. The initiation efficiency increased when the catalyst solution was added slowly to the initiator solution ([a]Matyjaszewski et al., 1998).

In ATRP, initiation is accomplished through homolytic cleavage of activated halogen-containing compounds and addition of the generated radicals to alkenes. The radical-stabilizing group should reside on the R-C atom (aryl, carbonyl, nitrile, multiple halogens) or involve weak bonding with heteroatoms (S, N, and O). Direct bonding of the halogen to an aryl or carbonyl group does not facilitate radical generation, and since vinyl, acyl halides, or haloarenes are bad ATRP initiators, ATRP can be carried out, e.g., in chlorobenzene. The fragment that forms the R-end of the polymer chain can contain a number of functional groups tolerant to ATRP catalysts and radicals.

4.2.1. Halogenated Alkanes

Halogenated alkanes, such as $CHCl_3$ or CCl_4, are typically used in atom transfer radical addition and were among the first studied as ATRP initiators (Dabrowski et al., 1999; Bourbigot et al., 2000). In the ruthenium-catalyzed ATRP of MMA, molecular weights of the polymer increased linearly with the conversion; however, at high monomer conversion, the molecular weight deviated from the theoretical values (Kotani et al., 1996). The polymers obtained were monomodal with low polydispersities (ca. 1.3). In contrast, di- or monochloromethanes were not able to polymerize MMA under similar conditions (Ando et al., 1997).

4.2.2. Benzylic Halides

Benzyl-substituted halides are useful initiators for the polymerization of styrene and its derivatives due to their structural resemblance. However, they fail in the polymerization of more reactive monomers in ATRP such as MMA. For example, using CuCl- dNbpy)$_2$ as the catalyst, inefficient initiation was observed when 1-phenylethyl chloride was employed as the initiator for the polymerization of MMA (108). pMMA with much higher molecular weights than the theoretic values and high polydispersities (*M*w/*M*n) 1.5-1.8) were obtained. In contrast, a well-controlled polymerization was realized with benzhydryl chloride (Ph_2CHCl) as the initiator under similar conditions. In fact, the radical generation was so fast that slow addition of benzhydryl chloride was necessary to avoid a significant contribution of irreversible biradical termination early in the polymerization ([e]Matyjaszewski et al., 1998). Improvement of the initiation efficiency for the ATRP of MMA using primary and secondary benzylic halides is possible by employing the halogen Exchange concept (Matyjaszewski et al., 1998).

4.2.3. α-Haloesters

Various α-haloesters have been successfully employed to initiate well-controlled ATRP. In general, α-haloisobutyrates produce initiating radicals faster than the corresponding α-halopropionates due to better stabilization of the generated radicals after the halogen abstraction step.

Thus, slow initiation will generally occur if α-halopropionates are used to initiate the polymerization of methacrylates. In contrast, α-bromopropionates are good initiators for the ATRP of acrylates due to their structural resemblance.

4.2.4. α -Haloketones

The stronger electron-withdrawing power of the ketone's carbonyl induces further polarization of the carbon-chlorine bond, which is attributed to the faster initiation observed with the ketones than with the ester counterparts.

An α-bromoketone has been used to initiate the controlled polymerization of MMA catalyzed by Ni{o,o'-$(CH_2NMe_2)_2C_6H_3$}Br (Granel et al., 1996) and $Ni(PPh_3)_4$ (Uegaki et al., 1999). Polyhalogenated α-haloketones (e.g., CCl_3COCH_3 and $CHCl_2COPh$) are among the best initiatorsfor the ATRP of MMA catalyzed by ruthenium complexes (Nishikawa et al., 1999; Ando et al., 1997; Takahashi et al., 1999; Ando et al., 1996 and Nishikawa et al., 1997). Well-controlled polymers with low polydispersities ($Mw/Mn < 1.20$) have been obtained.

4.2.5. α-Halonitriles

α-Halonitriles are fast radical generators in ATRP, due to the presence of the strong electron-withdrawing cyano group. Moreover, the

radical formed after halogen abstraction is sufficiently reactive, which leads to fast initiation through rapid radical addition to monomer. Of the initiators studied for the polymerization of acrylonitrile catalyzed by copper complexes, 2-bromopropionitrile resulted in polymers with the lowest polydispersities (Matyjaszewski et al., 1997). 2-Bromopropionitrile is also the initiator of choice when a bromine initiator is desired in the iron-mediated ATRP of MMA ([c]Matyjaszewski et al., 1997). However, α-halonitriles were not used in ruthenium-catalyzed ATRP as the cyano group deactivates the catalyst by forming a strong complex with ruthenium (Ando et al., 1997).

4.2.6. Sulfonyl Halides

As ATRP initiators, sulfonyl chlorides yield a much faster rate of initiation than monomer propagation (Percec et al., 1998). The apparent rate constants of initiation are about four (for styrene and methacrylates) and three (for acrylates) orders of magnitude higher than those for propagation. As a result, well-controlled polymerizations of a large number of monomers have been obtained in copper-catalyzed ATRP (Percec and Barboiu, 1995; Percec et al., 1998). End-functional polymers have been prepared using sulfonyl chlorides where functionalities were introduced onto the aromatic ring (Percec et al., 1997). The phenyl group substituent has only a small effect on the rate constant of initiation because the sulfonyl radical and its phenyl group are not related through conjugation. A unique feature of the sulfonyl halides as initiators is that

although they are easily generated, they only dimerize slowly to form disulfones and slowly disproportionate. Thus, they can react with the monomers and initiate the polymerization efficiently (Percec et al., 2000).

4.3. Transition Metal Complexes

Various transition metal complexes have been used in ATRP to generate growing radicals; the metal center should undergo an electron transfer reaction with the abstraction of a (pseudo) halogen and expansion of the coordination sphere. In addition, to differentiate ATRP from the conventional redox-initiated polymerization and induce a controlled process, the oxidized transition metal should rapidly deactivate the propagating polymer chains to form the dormant species.

The ideal catalyst for ATRP should be highly selective for atom transfer and should not participate in other reactions. It should deactivate extremely fast with diffusion-controlled rate constants, and it should have easily tunable activation rate constants to meet particular requirement for specific monomers. Thus, very active catalysts with equilibrium constants for styrenes and acrylates $K > 10^{-8}$ are not suitable for methacrylates. Polymerization of acrylamides requires higher activities (corresponding to $K > 10^{-7}$ for styrenes). Potential control of vinyl acetate and vinyl chloride may need catalysts with $K > 10^{-5}$ (for styrenes). These have not yet been developed. The overall thermodynamic activity defined by the equilibrium constant is not sufficient to define the utility of the

catalyst, and the aforementioned dynamics of exchange is of paramount importance. This requires facile rearrangement and expansion of the coordination sphere to accommodate incoming halogen. There is a correlation of the ATRP equilibrium constants and electrochemical redox potential for the outer-sphere electron transfer (OSET). However, the equilibrium constant depends also on the affinity of the complex to halogens. Thus, late transition-metal complexes are more reducing but have lower affinity to halogens. This may allow one to choose the appropriate complexes for different monomer groups to avoid side reactions associated with the oxidation and reduction of propagating free radicals.

The different transition metal complexes are represented following their periodic groups. But copper based system will be explained because of their synthetic versatility and low cost.

A series of lithium molybdate(V) complexes [LiMo- $(NAr)_2$(C-*N*)R] (C-*N*) $C_6H_4(CH_2NMe_2)$-2; R= (C-*N*), Me, CH_2SiMe_3, or *p*-tolyl), have been used in the ATRP of styrene using benzyl chloride as the initiator (Brandts et al., 1999).

Rhenium(V) iododioxobis(triphenylphosphine) ($ReO_2I(PPh_3)_2$) in the presence of Al- (O*i*Pr)$_3$ was reported to be an effective catalyst for the controlled polymerization of styrene using an alkyl iodide as the initiator (Kotani et al., 1999).

Different ruthenium-catalyzed ATRP was carried out. First reported by Sawamoto et al. in 1995 (Dabrowski et al., 1999). The others; (Ando et al., 1996; Nishikawa et al., 1999; Del Rio et al., 2000; [a]Simal et al., 1999; [b]Simal et al., 1999; Simal et al., 2000 and Ando et al., 2000).

$FeCl_2$, $FeCl_3$ and $FeBr_2$ are used in ATRP with different initiator and ligand. For example, $FeCl_2(PPh_3)_2$ complex is used with CCl_4 in toluene (Lecomte et al., 1997) , $FeBr_2$ catalyst system was used from Matyjaszewski et al. (Matyjaszewski et al., 1997), MMA has been polymerized $FeCl_3/PPh_3$ at 85 °C ([a]Moineau et al., 1998).

Different Rhodium systems heve been used recently. $RhCl(PPh_3)_3$ was used with a sulfonyl chloride for styrene polymerisation (Percec et al., 1996), $RhCl(PPh_3)_3$ was used in THF or a mixture of THF and H_2O ([b]Moineau et al., 1998).

Ni(0), Ni{o,o'-$(CH_2NMe_2)_2C_6H_3$}X (denoted as Ni(NCN)Br), $NiBr_2(PPh_3)_2$ complexes were used by researchers. References were shown respectively (Otsu et al., 1990; Percec et al., 1996; Granel et al., 1996 and Uegaki et al., 1997).

Nickel halides complexed by phosphorus ligands have also been used for the ATRP of MMA (Scheme 15) (Uegaki et al., 1997; Uegaki et al., 1998 and Moineau et al., 1999).

pMMA has been synthesized using $Pd(OAc)_2$ complexed by PPh_3 as the catalyst and CCl_4 as the initiator (Lecomte et al., 1997).

Copper which having a wide variety of skills and low cost is most common used catalyst for the ATRP. It was used polymerization for the styrenes, (meth)acrylate esters and amides, and acrylonitrile have been successfully polymerized using copper-mediated ATRP (Patten and Matyjaszewski, 1998; Matyjaszewski et al., 1999 and Patten and Matyjaszewski, 1999). The polymerization can be achievable monomers which have various functional groups, such as -OH and $-NH_2$, and insensitive to additives, such as H_2O, CH_3OH, and CH_3CN via copper catalyst ([d]Matyjaszewski et al., 1997). Regio- and chemoselectivities were done in this system. These properties provide control over the microstructure of the polymers and the end groups, the reactivity ratios, and the sensitivity to transfer agents (Wang et al., 1997; Granel et al., 1996 and Heuts et al., 1999).

Different polydentate ligands have been used for copper-mediated ATRP (Destarac et al., 1997; Cheng et al., 1999; Wang et al., 1999; Kickelbick and Matyjaszewski, 1999; Amass et al., 1999; Haddleton et al., 1997; Xia and Matyjaszewski, 1999 and Ando et al., 1997). These ligands have various advantages such as easily preparation and allowing for further modifications and tuning of the catalyst, promoted well-controlled polymerizations of styrene and (meth)acrylates (Xia and Matyjaszewski, 1999). Different counterions except halides have also

been used (Singha and Klumperman, 2000; Davis et al., 1999; [f]Matyjaszewski et al., 1998 and Woodworth et al., 1998).

The equilibrium constant is important in these reactions. Its values change about $K > 10^{-5}$ -1 0^{-8}. The equilibrium constant depends also on the affinity of the complex to halogens. Thus, late transition-metal complexes are more reducing but have lower affinity to halogens. This may allow one to choose the appropriate complexes for different monomer groups to avoid side reactions associated with the oxidation and reduction of propagating free radicals ([a]Matyjaszewski and Xia, 2001).

The ideal catalyst for ATRP should be highly selective for atom transfer and should not participate in other reactions. It should deactivate extremely fast with diffusion-controlled rate constants, and it should have easily tunable activation rate constants to meet particular requirement for specific monomers.

4.4. Ligand

The main role of the ligand in ATRP is to solubilize the transition-metal salt in the organic media and to adjust the redox potential of the metal center for appropriate reactivity and dynamics for the atom transfer (Xia et al., 2000). There are several guidelines for an efficient ATRP catalyst. First, fast and quantitative initiation ensures that all the polymer chains start to grow simultaneously. Second, the equilibrium between the

alkyl halide and the transition metal is strongly shifted toward the dormant species side. This equilibrium position will render most of the growing polymer chains dormant and produce a low radical concentration. As a result, the contribution of radical termination reactions to the overall polymerization is minimized. Third, fast deactivation of the active radicals by halogen transfer ensures that all polymer chains are growing at approximately the same rate, leading to a narrow molecular weight distribution. Fourth, relatively fast activation of the dormant polymer chains provides a reasonable polymerization rate. Fifth, there should be no side reactions such as β-H abstraction or reduction/oxidation of the radicals.

4.4.1. Nitrogen Ligands

Nitrogen ligands have been used in copper- and iron-mediated ATRP (117,150). Activity of N-based ligands in ATRP decreases with the number of coordinating sites N4 > N3 >N2 . N1 and with the number of linking C-atoms C2 > C3. C4. It also decreases in the order R_2N- > R-Nd > Ph-Nd > Ph-NR-. Activity is usually higher for bridged and cyclic systems than for linear analogues.

4.4.2. Phosphorus Ligands

Phosphorus-based ligands are used to complex most transition metals studied in ATRP, including rhenium, ruthenium (Kato et al., 1995

and [a]Simal et al., 1999), iron (Matyjaszewski et al., 1997 and Ando et al., 1997), rhodium (Percec et al., 1996 and [b]Moineau et al., 1998), nickel (Uegaki et al., 1997 and Uegaki et al., 1998) and palladium (Lecomte et al., 1997).

4.4.3. Miscellaneous Ligands

A few ligands have been used with ruthenium in ATRP system. For example; Cyclopentadienyl (Takahashi et al., 1999), indenyl (Ando et al., 2000) and 4-isopropyltoluene ([a]Simal et al., 1999).

Ligands are the most important component for the ATRP. They can fine-tune selectivities and force the complex to participate in a one electron transfer process needed for ATRP in comparison with the preferred two-electron-transfer process, such as oxidative addition and reductive elimination for Ni or Pd complexes. Ligands serve several purposes. In addition to primary roles of tuning atom transfer equilibrium constants and dynamics as well as selectivities, they control solubilities in the reaction mixture and ensure stability of the complexes in different monomers, solvents, and temperatures. This is especially important in polymerization of acidic monomers and monomers which can strongly complex transition metals such as pyridine-, amide-, or amine-containing monomers. Proper design of ligands is especially important in polymerization under heterogeneous conditions, in water or ionic liquids. Partition coefficients and their dependence on temperature will define the

efficiency of the catalyst for ATRP. Ligands may also facilitate the removal and recycling of the catalyst. They may allow the immobilization of the catalyst and also distribution between two phases. There are many redox-active enzymatic systems ([a]Matyjaszewski and Xia, 2001).

4.5. Additives

ATRP can be accelerated with adding some additives. When a small amount of copper (0) was added to the styrene and (meth)acrylates ATRP systems, a significant rate increase was observed ([a]Matyjaszewski et al., 1997 and Cheng et al., 1999). Copper (0) reduces the concentration of copper(II) and simultaneously increased the concentration of copper(I). The addition of iron powder to salts of Fe(II) or Fe(III) resulted in a similar increased rate of polymerization (Matyjaszewski et al., 1997). If some reducing agents such as sugars and aluminum alkoxides are added similar effect can be observed (Guo et al., 2000). Moreover, if a sufficient amount of zerovalent metal is present, the controlled radical polymerization can be carried out without the removal of any oxygen or inhibitor ([c]Matyjaszewski et al., 1998).

5. MATERIALS & METHODS

5.1 Materials

Triethylamine (Sigma-Aldrich), 6-amino haxanol (Fluka), pyridine (Sigma-Aldrich), acetone, KOH, NaOH, 1,6-diaminohexane (Sigma-Aldrich), dibenzoylperoxide, p-hyroxy benzaldehyde, 5-bromopentyl) threemethylammonium bromide (Sigma-Aldrich), dichloro methane, benzyl chloroformate (CBZ) (Fluka), trifluoroacetic acid (TFA) (Sigma-Aldrich), ethylenediamine (Fluka), ethanol, di-tert-butyldicarbonate (BOC) (Sigma-Aldrich), methyl iodide, α, α'-dichloro-p-xylene (Sigma-Aldrich), cetyltrimethylammonium bromide (CTAB), p-Toluenesulfonic acid. 2-Bromoisobutyryl bromide (Sigma-Aldrich) was vacuum distilled. Methyl ethyl ketone (MEK) and 1-propanol were purified by distillations over CaH_2. Bpy (2, 2'-Bipyridine) from Aldrich was recrystallized from *n*-hexane to remove impurities. CuBr was washed with acetic acid followed by methanol to remove impurities. All of the chemicals are reagent grade.

Purification of the monomer was done as follows. The first procedure involved washing an aqueous solution (25 vol % HEMA) of monomer with hexanes (4 x 200 mL), salting the monomer out of the aqueous phase by addition of NaCl, drying over $MgSO_4$, and distilling under reduced pressure. We used Montmorillonite K10(Sigma-Aldrich) in our studies. It has surface area: 220-270 m^2/g, pore volume 0,318 ml/g (at nm range by CCl_4) and bulk density 300-370 g/l.

The chemical analysis of montmorillonite was determined with X-Ray Floresance Spectrometer. The results of chemical analysis of the major elements for the montmorillonite are shown in table 5.1

Table 5.1. Chemical Analysis of the Main Elements of the Montmorillonite Minerals

	Montmorillonite (K10) %
SiO_2	66.65
Al_2O_3	14.42
Fe_2O_3	3.46
MgO	1.60
Na_2O	0.21
CaO	0.23
K_2O	2.19
SO_3	0.21

Chemical reagents, solutions and products were characterized with NMR and FTIR. Molecular weight and molecular weight distribution of the polymers were determined via GPC. The structure of nanocomposites typically was proved using X-ray diffraction (XRD) analysis and transmission electron micrographic (TEM) images. Both TEM and XRD are essential tools for evaluating nanocomposite structure. Basically XRD studies yielded quantitative characterization of nanostructure and TEM gives qualitative information about the nanostructure.

5.2 Methods

Two types of the polymerisation methods were used to synthesis of the pHEMA. First is radically polymerisation with Dibenzoylperoxide, second is polymerisation via ATRP.

In the case of initiator synthesis and after the polymerization products were characterized by ^{1}H-NMR and ^{13}C-NMR using a VARIAN 400 NMR spectrometer. Various deuterated solvents were used as the solvent and the measurements were taken at room temperature.

We also used FTIR (Perkin Elmer Pyris 1) spectroscopy to understand the structure of the initiator, modified montmorillonite and nanocomposites. FTIR by itself not enough to identify the products and must be accompanied by other techniques.

The reasons of easiness and availability XRD is most commonly used to probe the nanocomposite structure and to identify expansion of clay plateles. In this method, the sample preparation is relatively easy and the X-ray analysis can be performed within a few hours.

This method was used in our studies to determine the interlayer spacing of the silicate layers for unmodified, modified MMT (K10) and description type of the nanocomposites. XRD diagrams were taken from a Phillips E'xpert Pro in "İzmir Yüksek Teknoloji Enstitüsü".

Molecular weight and molecular weight averages are affective parameters of physical properties on polymers. For that reason these parameters are important.

Before the GPC measurement, the polymer was cleaved from clay by refluxing the nanocomposite in MEK/1-propanol saturated solution (80/20, v/v) of p-Toluenesulfonic acid.

TEM allows a qualitative understanding of the internal structure, spatial distribution of the various phases, and views of the defect structure through direct visualization.

This method was used in our studies to description type of the nanocomposites. TEM images diagrams were taken from a Jeol 6355 in "Tubitak MAM".

The measurement of Tg was performed on a Universal V4.3A TA Instrument DSC instrument. The DSC trace was recorded upon heating at a rate of 10 °C/min. All of the products were dried in an evacuated oven at 55^0C on 10 mbar pressure before the thermal analyses.

TGA thermograms were taken from a Perkin Elmer Pyris 1 TGA/DTA instrument analyzer at heating rate of $15^0 Cmin^{-1}$ under a 10 bar dry air atmosphere and Nitrogen between 50 and 750 ^{0}C. All of the

products were dried in vacuum oven at 55^0C on 10 mbar pressure before the thermal analyses.

6. RESULTS AND DISCUSSION

6.1. Initiator Synthesis and Characterization

Various reaction systems were tried to synthesis the initiator. These systems were explained as below. All of the names of the products were done according to IUPAC.

6.1.1. Synthesis of 6-[(2-bromo-2-methylpropanoyl)amino]hexan-1-aminium bromide

We planned to synthesis an initiator which have both cation and initiator moiety for this reaction. Reaction was carried out according to (Zhao[b] et al., 2003) for this aim.

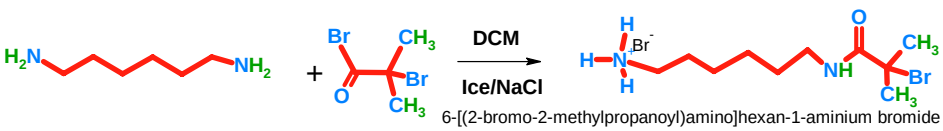

Figure 6.1. Initiator Synthesis Process for 6,1,1

Mono initiator added diamine reaction was tried by dissolving 1.1 g of 6-aminohexylamine in 4 ml of dry DCM. 2.34 ml of 2-Bromoisobutyryl bromide was dissolved in 5ml anhydrous DCM. This solution transferred to a dropping funnel. This 2-bromoisobutyryl bromide solution was dropwise added in 1h. After stirring the mixture for

20 h, solvent was evaporated. Various solvents were tried to purification of this monoquaternized product with initiator.

If peak area in ^{1}H NMR spectrum was investigated, not mono but di adding of the 2-bromoisobutyryl bromide to 6-aminohexylamine can be seen. This result indicates that mono adding of amine did not take placed.

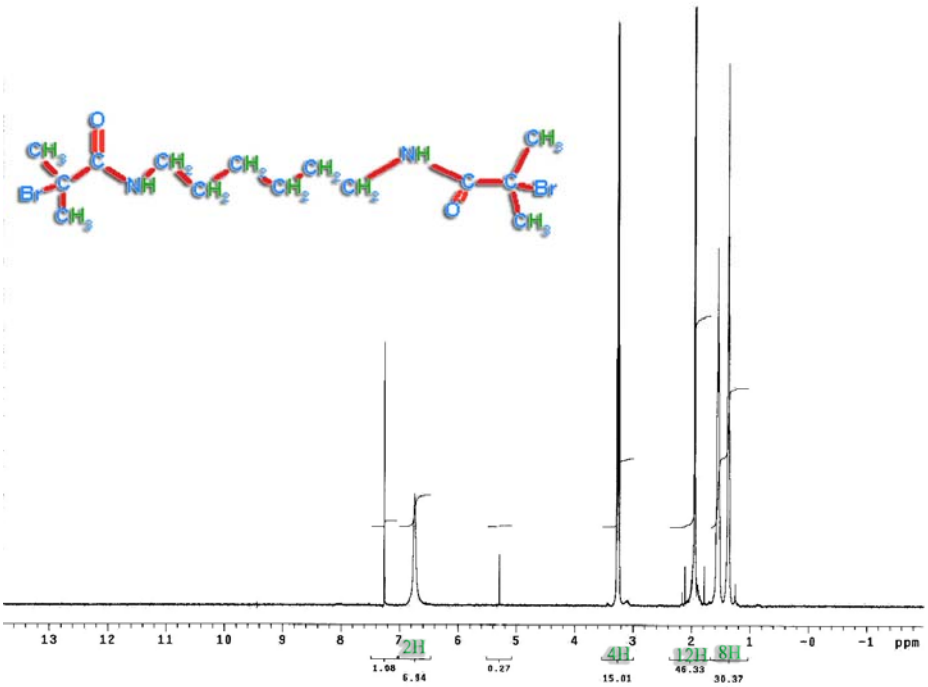

Figure 6.2. ^{1}H NMR Spectrum Of Product For Reaction 6.1.1

Peak areas were calculated and protons were signed in figure 6.2. By adding protons, we can clearly see that the isolating product is diprotecting group.

6.1.2 Synthesis of N-[4-(chloromethyl)benzyl]-N,N-diethylethan aminium chloride

We planned to synthesis an initiator which have both cation and initiator moiety for this reaction. The reaction was carried out according to (Zhao[b] et al., 2003) for this aim.

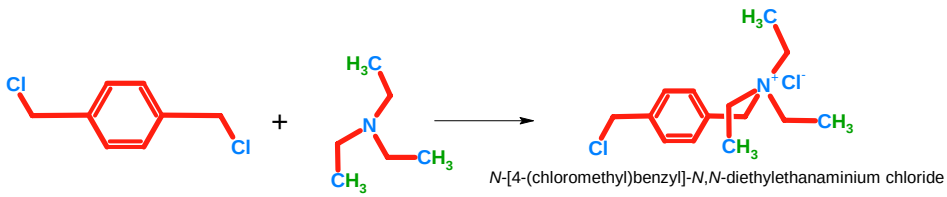

Figure 6.3. Initiator Synthesis Process for 6,1,2

The synthesis of initiator which have both quaterner amine and ATRP initiator moiety was tried by dissolving 0.7 g of α, α'-Dichloro-p-xylene in 10 ml of dry DCM. 0.39 ml of TEA was dissolved in 5ml anhydrous DCM. This solution was transferred to a dropping funnel. This TEA solution was dropwise added in 1h. After stirring the mixture for 48h, the solvent was evaporated. Various solvents were tried for purification of this monoquaternized product with initiator.

After the reaction α,α'-p-Chloro xylene with TEA, aromatic C-H, aliphatic C-H and N^+ peaks appearance can be seen in figure 6.4. These are indicating that the reaction occurred but products (mono or diquaternized products) can not be isolated with high yield. For that reason we passed to next reaction system.

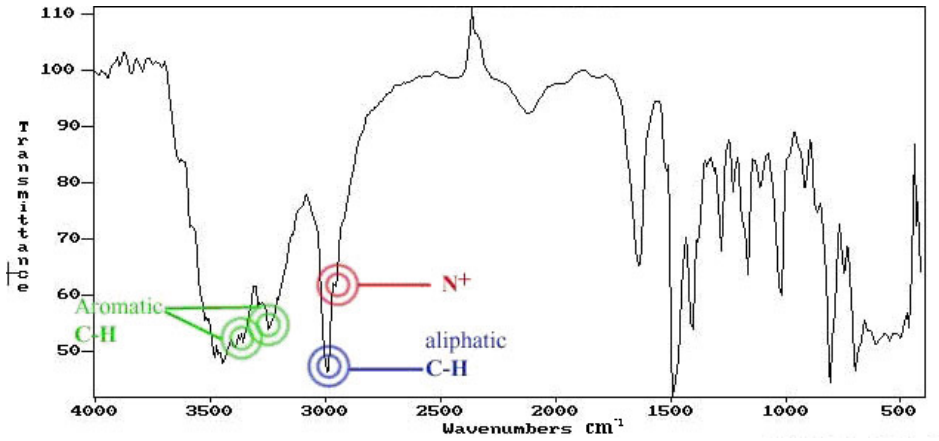

Figure 6.4. FTIR Spectrum of N-(-4(chloromethyl)Benzyl)-N,N-diethylethanaminium chloride

6.1.3. Synthesis of 6-[(2-bromo-2-methylpropanoyl) oxy]-N-methylhexan-1-aminium iodide

Our aims for these reaction systems are firstly mono quaternization of diamine and then adding initiator to other free amine group. These reactions were done according to (Chen et al., 2004) and (Zhao[b] et al., 2003).

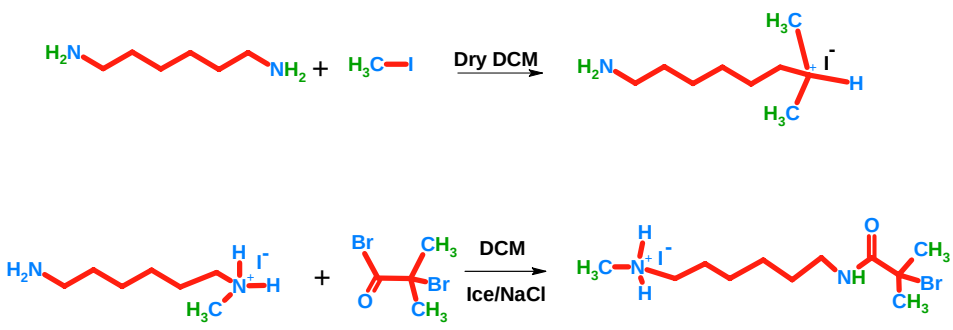

Figure 6.5. Initiator Synthesis Process for 6,1,3

Mono quaternization was tried by dissolving 0.5 g of 6-aminohexylamine (8.3 mmol) in 25 ml of dry DCM. A solution of methyl iodide (0.26 ml, 4.15 mmol) in dry DCM (5ml) was added under vigorous stirring and argon over a period of 24 hours. Various solvents were tried for purification of this monoquaternized product.

If FTIR spectrum of the a is compared with b in figure 6.6 , new N^+ peak at 2800 cm^{-1} appearance can be seen. This result indicated that quaternization of amine was done but because of the resulting product could not be isolated in high yield we desisted from this procedure.

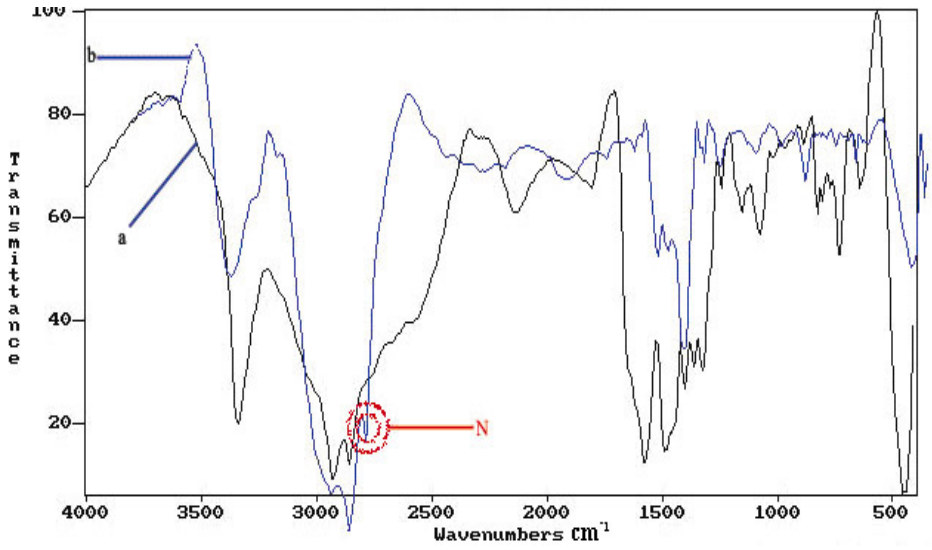

Figure 6.6. FTIR Spectra (a) 6-aminohexylamine (b) **6**-amino-*N*-methylhexan-1-aminium iodide

6.1.4. Synthesis of 6-[(2-bromo-2-methylpropanoyl) oxy]-N-methylhexan-1-aminium

These reactions were carried out according to the procedures reported by (Kofoed et al., 2001), (Zhao[b] et al., 2003) and (Hay et al., 2003).

6-aminohexylamine is the initial reactant for the synthesis. This mechanism consists of three steps: The first step is protecting one of the amine groups. The second step is adding initiating group to structure and last step is quaternization of the protecting amine group.

6-aminohexylamine (0.5 g, 8.3 mmoll) was dissolved in 5 ml of dry DCM. A solution of di-*tert*-butyldicarbonate (1.81 g, 8.3 mmol) in dry DCM (5ml) was added under vigorous stirring and argon over a period of 1 h. The reaction mixture was stirred for 1 h while cooling with water to 20°C. Water (5 ml) was slowly added to the reaction mixture over a period of 45 min. The mixture was stirred for another 15 min before phase separation and removal of the water phase. Water (10 ml) was added and the pH was adjusted to 1.5 with conc. HCl. The mixture was stirred for 15 min followed by phase separation and removal of the organic phase. DCM (10 ml) was added and the pH adjusted to 12 with 28% NaOH solution. The mixture was stirred for 15 min before removal of the organic phase. The water phase was extracted with DCM (3x7 ml) and the combined organic phases were evaporated to dryness *in vacuo*.

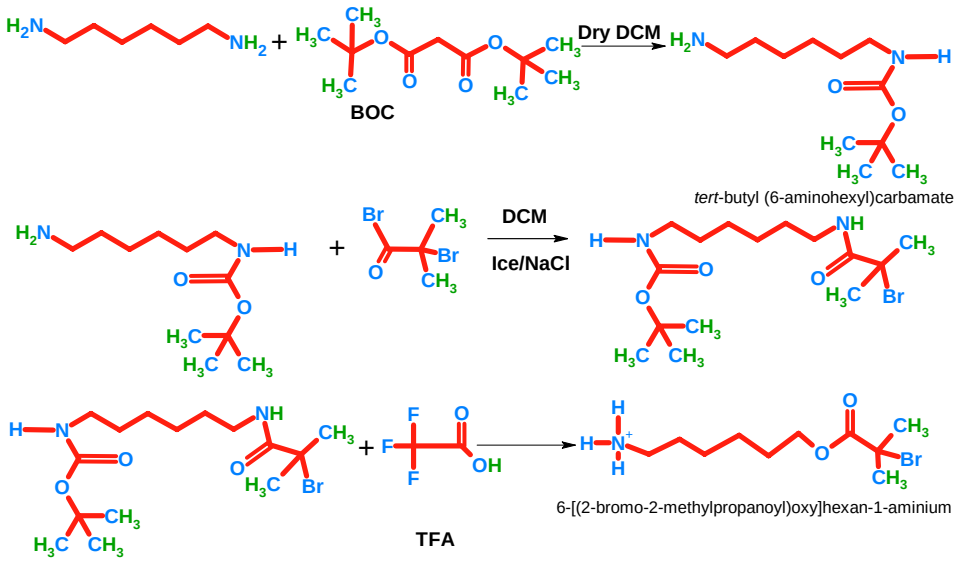

Figure 6.7. Initiator Synthesis Process for 6,1,4

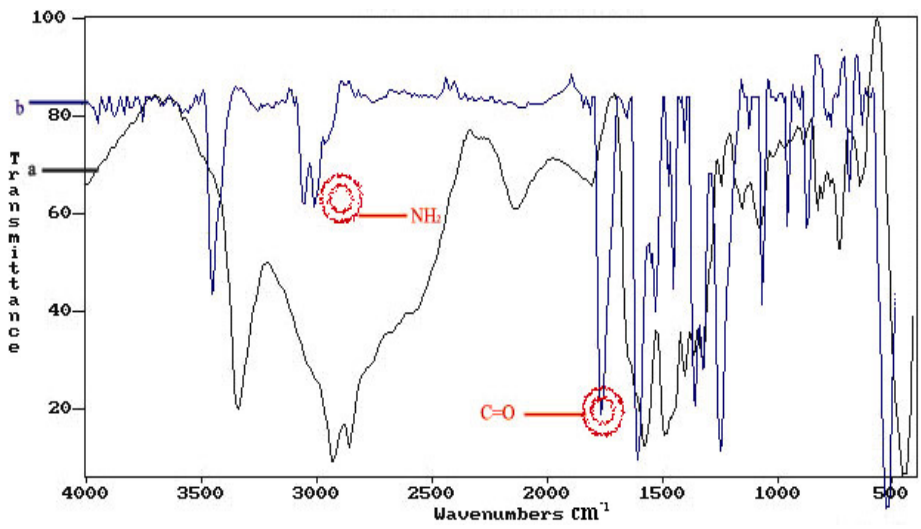

Figure 6.8. FTIR Spectra (a) 6-aminohexylamine (b) tert-butyl (6-aminohexyl)carbamate

According to FTIR spectra, we can clearly see both of C=O and NH_2 peaks. These results prove mono protection of the diamine group. However, the peak area in ^{1}H NMR spectrum indicates that, the products amounts were not enough to react with each other.

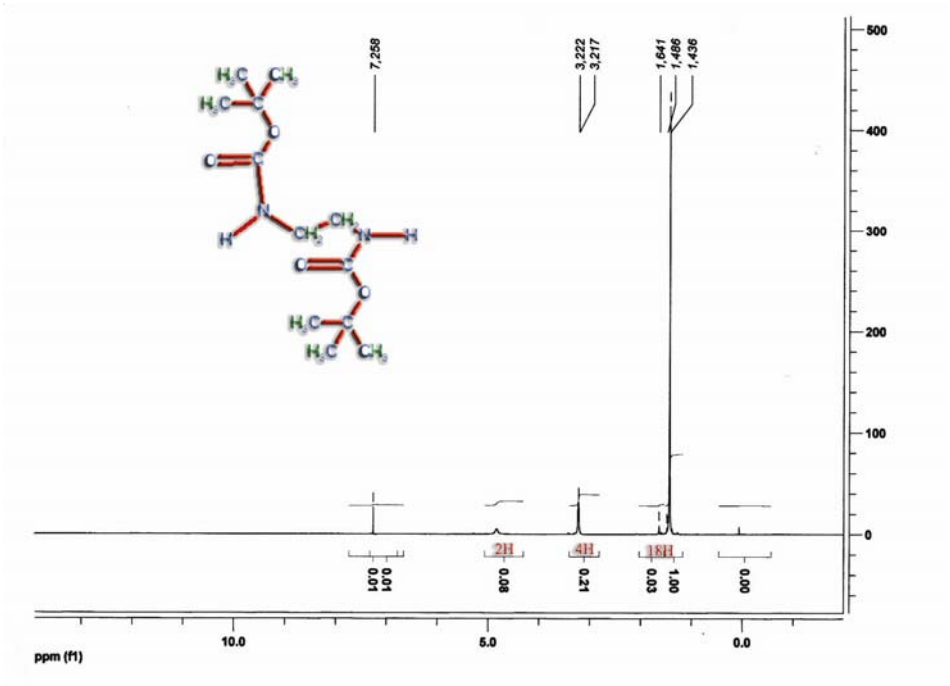

Figure 6.9. ^{1}H NMR Spectrum tert-butyl (6-aminohexyl)carbamate

6.1.5 Synthesis of 2-[(2-bromo-2-methylpropanoyl)amino] ethanaminium

These reaction systems have the same previous principle. The reactions were carried out according to the procedures reported by (Kofoed et al., 2001), (Zhao[b] et al., 2003) and (Hay et al., 2003).

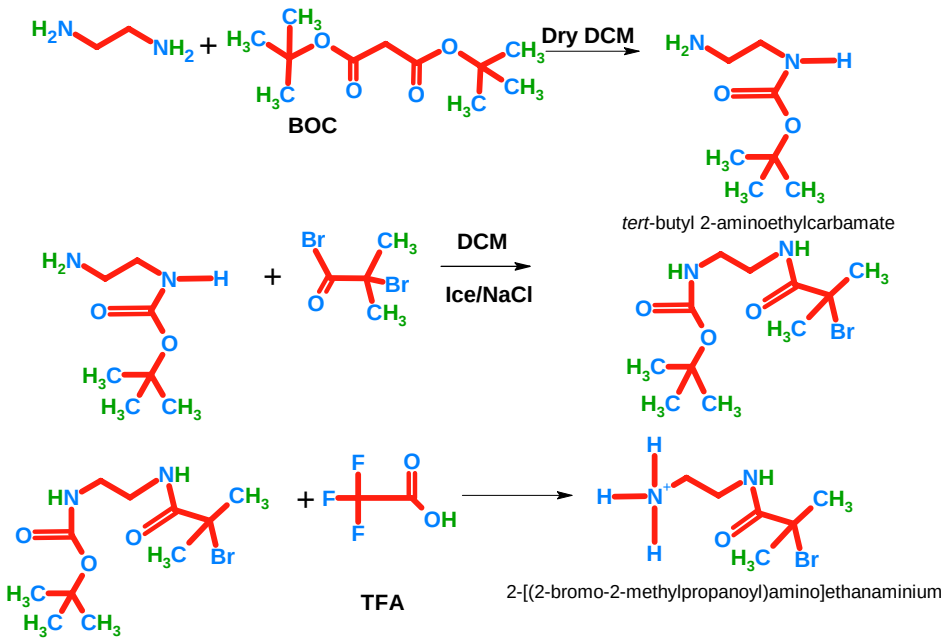

Figure 6.10. Initiator Synthesis Process for 6,1,5

2-aminoethylamine (0.6 ml, 8.3 mmoll) was dissolved in 3 ml of dry DCM. A solution of di-*tert*-butyldicarbonate (1.81 g, 8.3 mmol) in dry DCM (5ml) was added under vigorous stirring and argon over a period of 1 h. The reaction mixture was stirred for 1 h while cooling with water to 20°C. Water (5 ml) was slowly added to the reaction mixture over a period of 45 min. The mixture was stirred for another 15 min before phase separation and removal of the water phase. Water (10 ml) was added and the pH was adjusted to 1.5 with conc. HCl. The mixture was stirred for 15 min followed by phase separation and removal of the organic phase. DCM (10 ml) was added and the pH adjusted to 12 with 28% NaOH solution. The mixture was stirred for 15 min before removal

of the organic phase. The water phase was extracted with DCM (3x7 ml) and the combined organic phases were evaporated to dryness *in vacuo*.

The evaluation of FTIR spectra in figure 6.11 revealed that the intensity of NH_2 peak decreased and a new C=O peak has appeared. These results indicated that mono protection of 2-aminoethylamine was carried out. Because of the isolation problem of the desired product we stopped running this process.

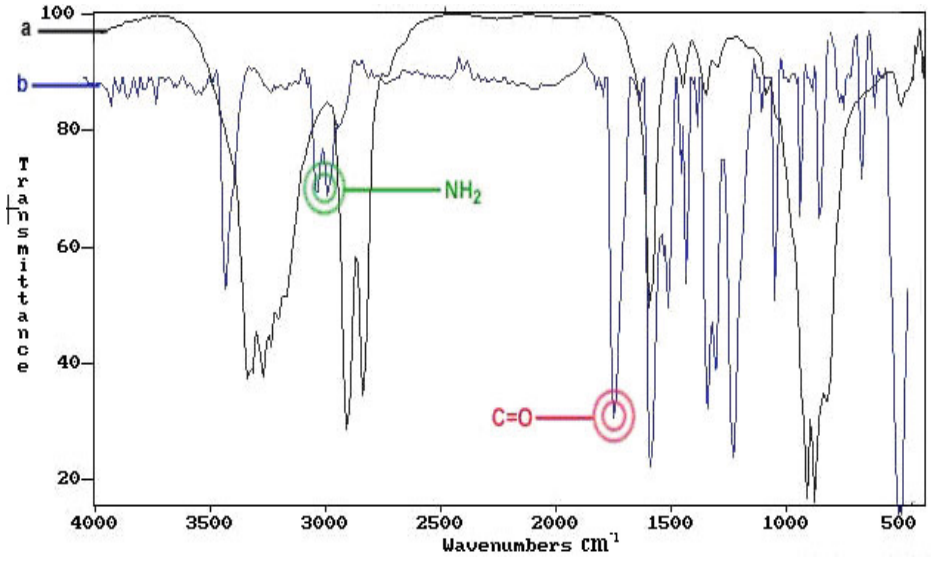

Figure 6.11. FTIR Spectra (a) 2-aminoethylamine (b) *tert*-butyl 2-aminoethylcarbamate

6.1.6. Synthesis of 6-[(2-bromo-2-methylpropanoyl)oxy]hexan-1-aminium

This reaction is based on the same previous procedure. Only the initial reactant was changed, CBZ was used instead of BOC. These reactions were done according to (Pittelkow et al., 2002), (Zhao[b] et al., 2003) and (Asayama et al., 2001).

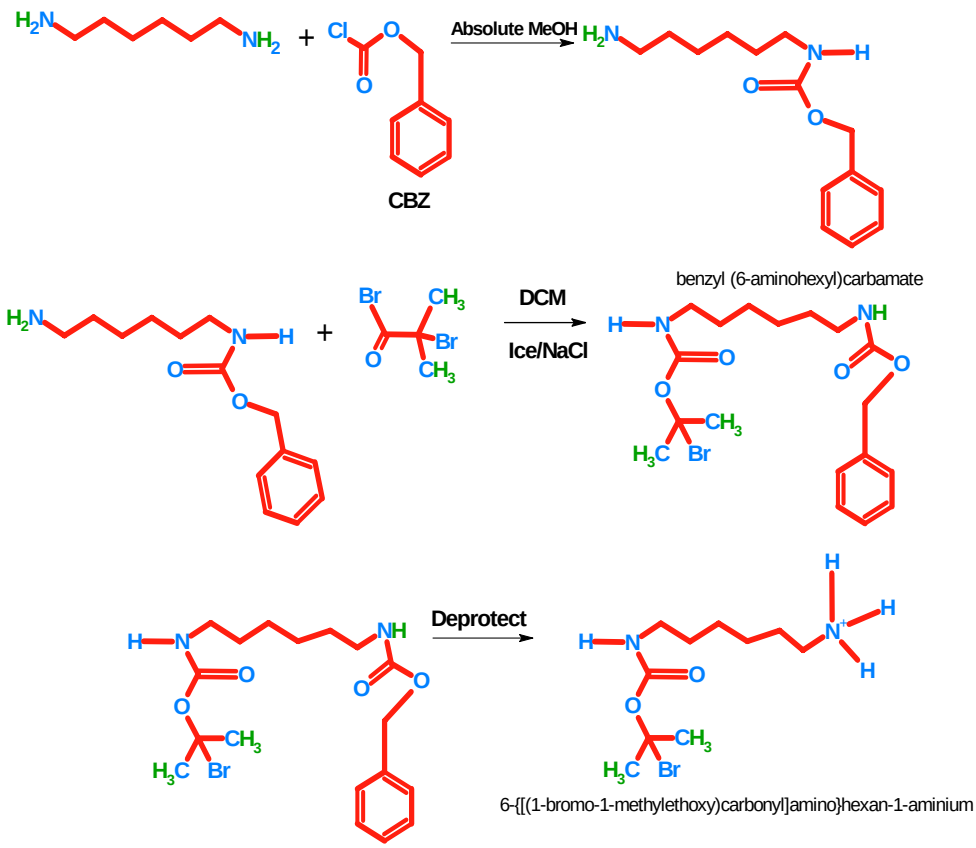

Figure 6.12.. Initiator Synthesis Process for 6,1,6

6-aminohexylamine is initial reactant for the synthesis. This mechanism consists of three steps: The first step is protecting one of the amine groups. The second step is adding an initiating group to the structure and the last step is the quaternization of the protecting amine group.

CBZ is another protecting group for protect of the diamines. For that reason CBZ was used in our system.

0.43 g of CBZ (2.5 mmol) is added to a stirring solution of 1,6-Diaminohexane (2.5 mmol) in absolute EtOH (5 mL). The reaction mixture was stirred over night at r.t. followed by removal of the volatiles in vacuo. H_2O (25 mL) was added and the pH adjusted to 3 by addition of aqueous HCl (2 M) followed by extraction with DCM (2 x 5 mL). The aqueous phase was then made strongly alkaline by addition of aq NaOH (2 M) and extracted with DCM (3 x 8 mL). The organic phase was dried using (Na_2SO_4), filtered and concentrated in vacuo.

When FTIR spectrum of the a is compared with b in figure 6.13, both C=O and aromatic C-H peaks can be seen. This result is indicated that the mono protection of amine was achieved, but because of the resulting product could not be isolated in high yield we desisted from this procedure.

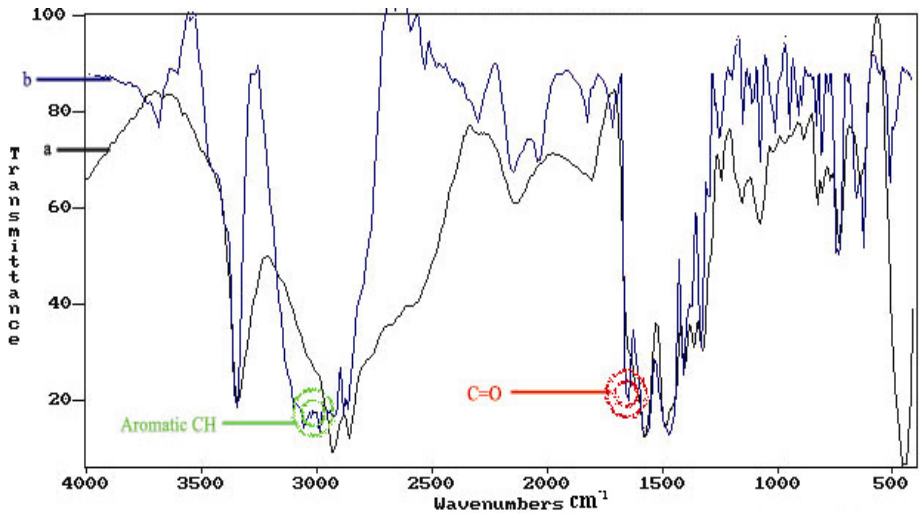

Figure 6.13. FTIR Spectra (a) 6-aminohexylamine ; (b) benzyl (6-aminohexyl) carbamate

6.1.7. Synthesis of 4-{[(6-aminohexyl)imino]methyl}phenol

Formation of the schiff base reaction is the initial reaction for this reaction system. These reactions were carried out according to main Schiff Base reaction, (Zhao[b] et al., 2003) and quaternization of amine group.

6-aminohexylamine (0.72 g, 6.2 mmol) was dissolved in 10 ml of ethanol. After the 0.756 g of p-hydroxy benzaldehyde was dissolved in 5 ml of ethanol. It was added to the previous solution in 1h. This solution was stirred at room temperature then half of this solution was transfered and investigated. The other part was refluxed for 1 day and analyzed.

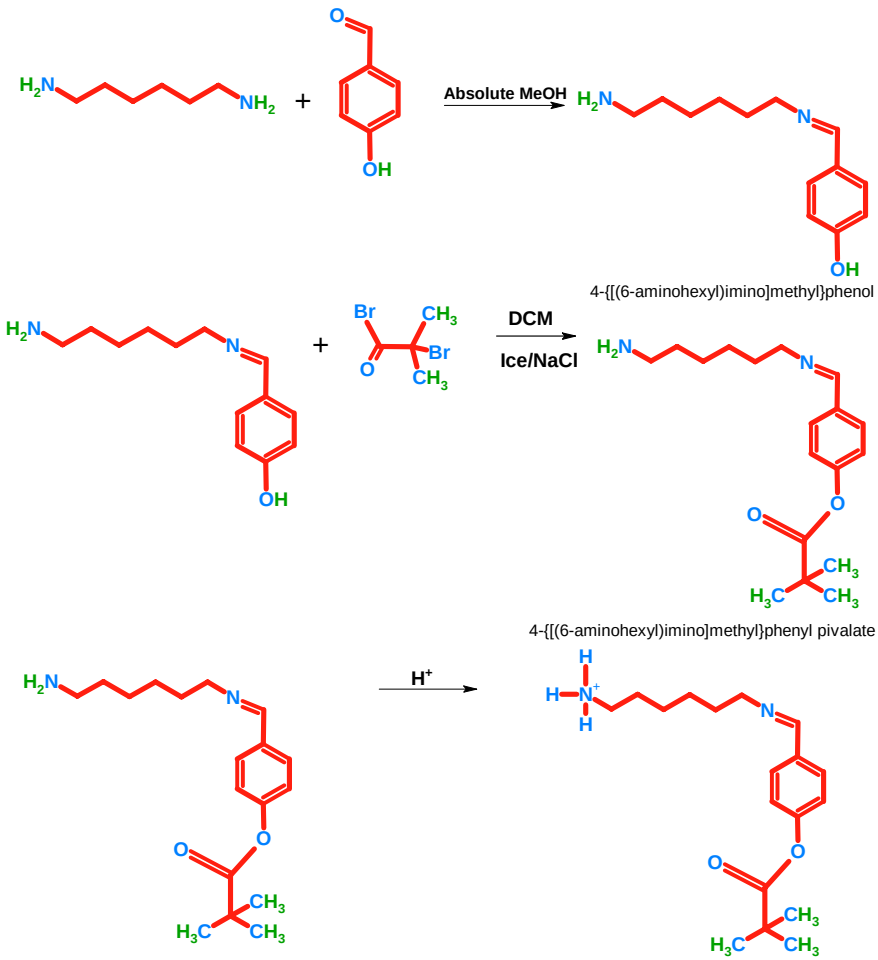

Figure 6.14. Initiator Synthesis Process for 6,1,7

Products could not be isolated.

6.1.8. Synthesis of 4-{(Z)-[(4-bromophenyl)imino]methyl}phenol

The schiff base reaction is an initial reaction for this reaction system. These reactions were done according to main Schiff Base

reaction, second esterification (Zhao[b] et al., 2003) and quaternization of amine group.

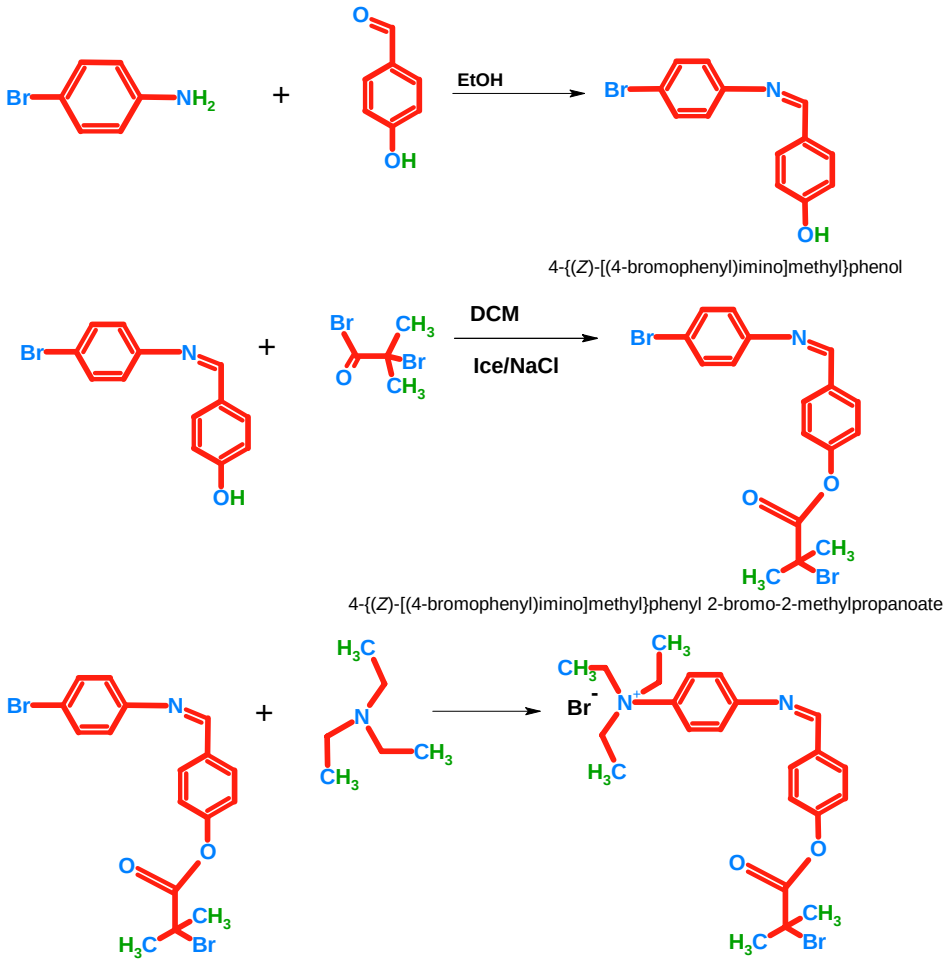

Figure 6.15. Initiator Synthesis Process for 6,1,8

6-aminohexylamine (0.9 g, 5.2 mmol) was dissolved in 10 ml of ethanol. After the 0.63 g of p-hydroxy benzaldehyde (5.2 mmol) was dissolved in 10 ml of ethanol. It was added to the previous solution in 1h.

This solution was stirred at room temperature and reflux at 65 ^{0}C for1 day. The products were purified and investigated.

If FTIR spectrum of a is compared with the b, new OH peak at 3490 cm^{-1} and C=N peak at 1630 cm^{-1} appearance can be seen. These are indicative that Schiff base reaction could be performed but because the resulting product could not be isolated in high yield, we desisted from this procedure.

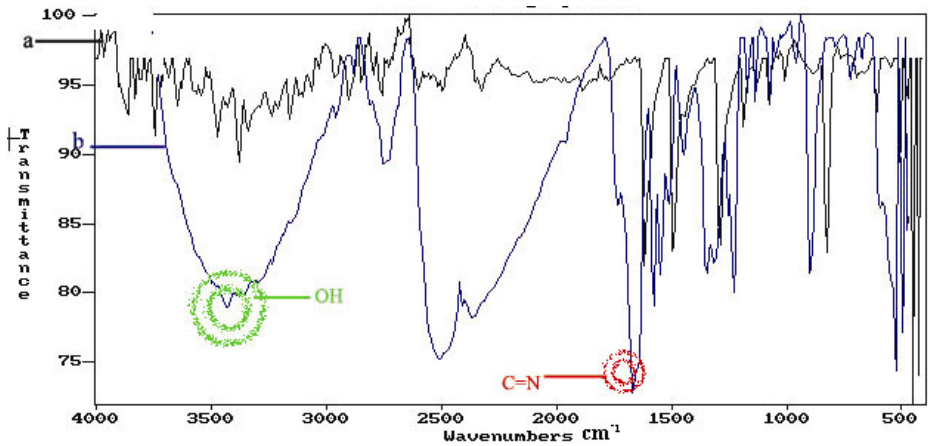

Figure 6.16. FTIR Spectra (a): p-Bromoanyline; (b)**:** 4-{(*Z*)-[(4-bromophenyl)imino]methyl}phenol; (c) 4-{(*Z*)-[(4-bromophenyl) imino]methyl}phenyl 2-bromo-2-methylpropanoate

6.1.9. Synthesis of 6-[(2-bromo-2-methylpropanoyl)oxy]-N,N,N-trimethylhexan-1-aminium bromide

(5-Bromopentyl)trimethylammonium bromide is the initial reactant for the synthesis. The first part is the substition reaction between

bromide and hydroxyl group. The second part is esterification of hydroxyl group using 2-bromoisobutyryl bromide (Zhao[b] et al., 2003).

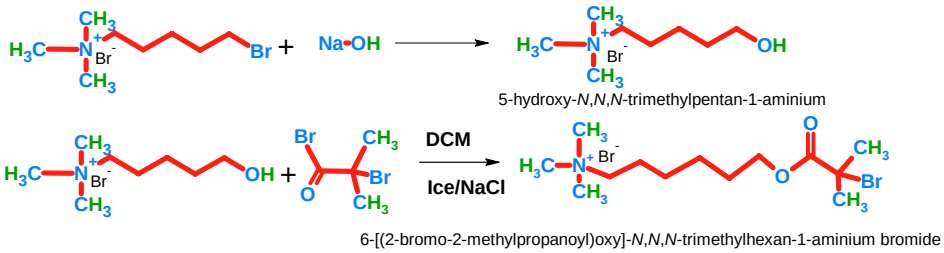

Figure 6.17. Initiator Synthesis Process for 6,1,9

1.0g of (5-Bromopentyl)trimethylammonium bromide is dissolved in 5ml methanol/acetone. 0.38 g of KOH is dissolved in the same solvent system too. This solution is added dropwise to previous solution in 1 h. White KBr product is removed with filtration and half of the solvent in which residue solution is removed in *vacou*. Finally product is precipitated in diethylether.

The esterification process with 2-bromo-isobutyryl bromide was explanined as below.

1.61g of 5-hydroxy-*N,N,N*-trimethylpentan-1-aminium bromide was dissolved in 10 ml anhydrous Acetone. The resulting solution was cooled in an ice bath and stirred for 0.5h and 1.42 ml of TEA was added. 1.11 ml of 2-Bromoisobutyryl bromide was dissolved in 5ml anhydrous acetone. This solution was transferred to a dropping funnel. This 2-bromoisobutyryl bromide solution was dropwise added in 3h. After

stirring the mixture for 20 h, the solvent was evaporated. Pyridine was used instead of TEA as a base in the same conditions. Various solvent-precipitated pairs were tried for isolation and purification for the product.

If FTIR spectrum of the a is compared with b, new OH peak at 3490 cm^{-1} appearance can be seen. According to figure 6.18, the OH peak can be easily seen at 2.69 ppm. These are proof of the hydroxsilation of the initial reactant. If spectrum b is compared with c, new carbonyl peak at 1730 cm^{-1} appearance and a decrease in intensity of the OH peak can be seen. These results showed that esterification process was achieved. Because the resulting product could not be isolated in high yield we desisted from this procedure.

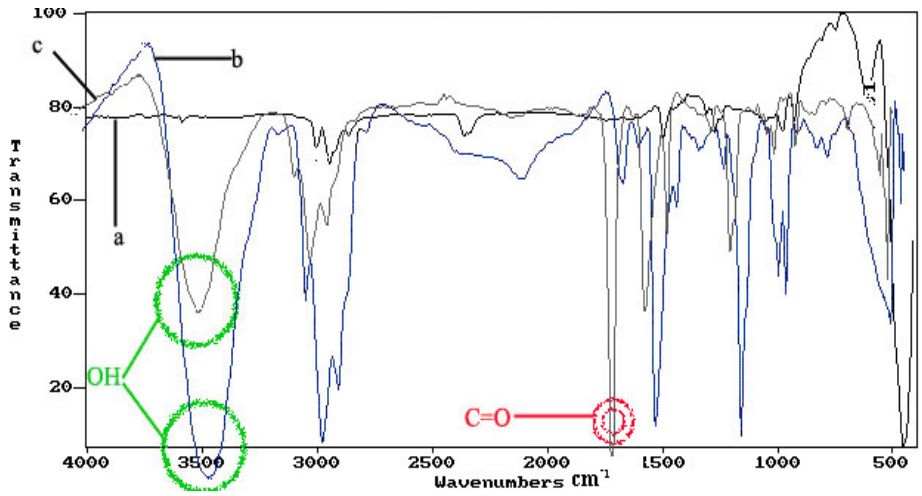

Figure 6.18. FTIR Spectra (a): (5-Bromopentyl) trimethylammonium bromide; (b); 5-hydroxy-*N*,*N*,*N*-trimethylpentan-1-aminium (c): 6-[(2-bromo-2-methylpropanoyl)oxy]-*N*,*N*,*N*-trimethylhexan-1-aminium bromide

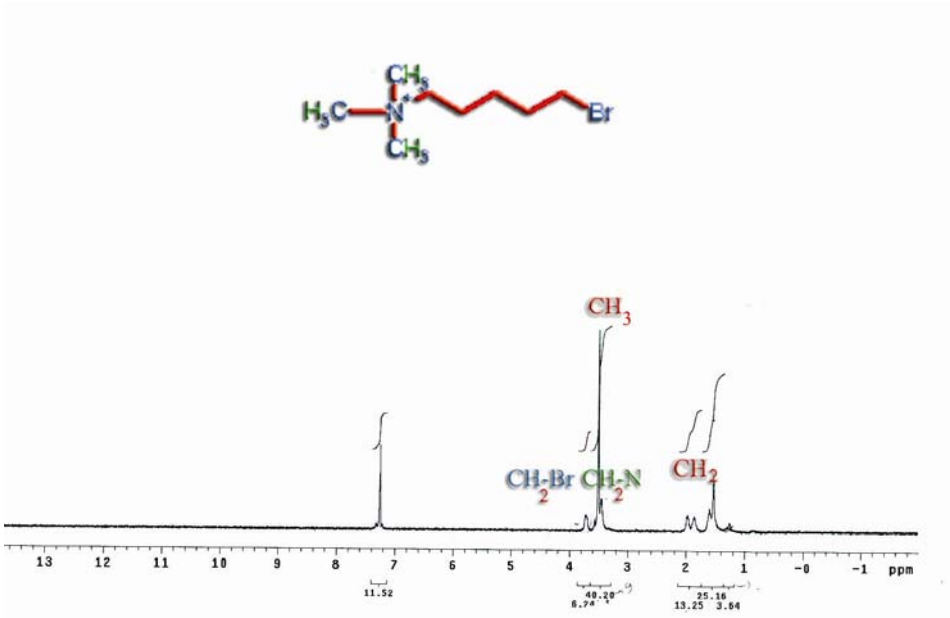

Figure 6.19. [1]H NMR Spectrum (5-Bromopentyl) trimethylammonium bromide;

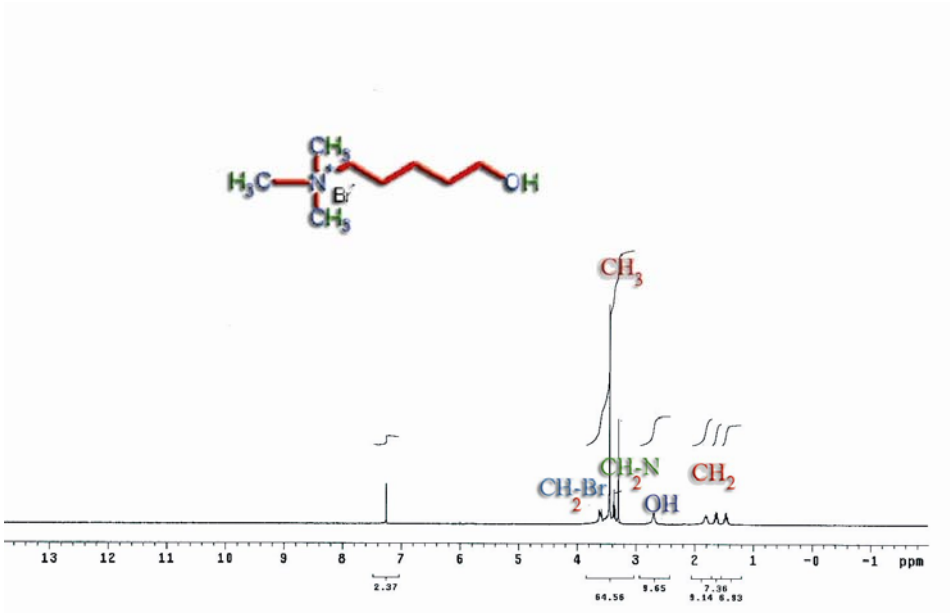

Figure 6.20. [1]H NMR Spectrum 5-hydroxy-*N*,*N*,*N*-trimethylpentan-1-aminium

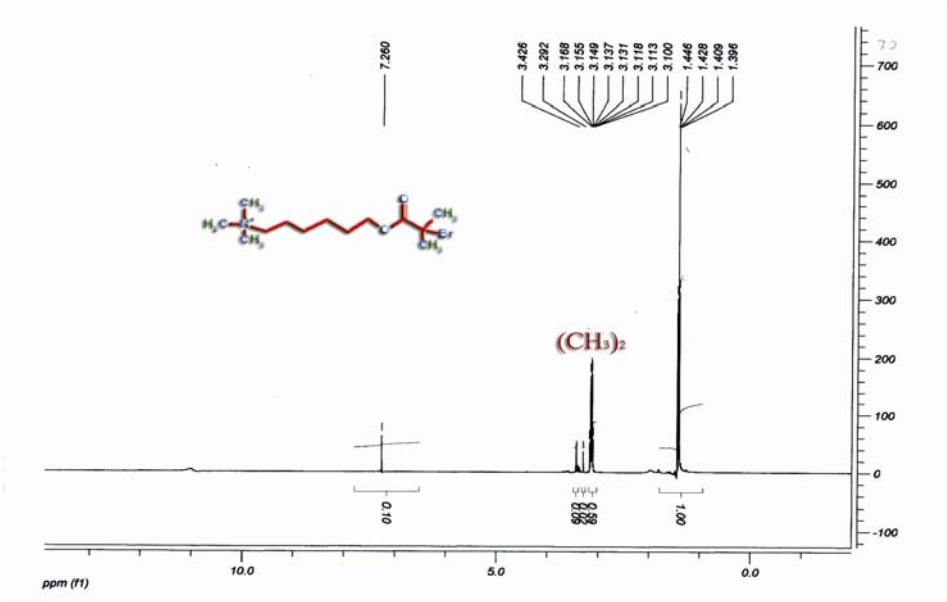

Figure 6.21. ^{1}H NMR Spectrum 6-[(2-bromo-2-methylpropanoyl)oxy]-*N*,*N*,*N*-trimethylhexan-1-aminium bromide

6.1.10. Synthesis of 6-[(2-bromo-2-methylpropanoyl)oxy]hexan-1-aminium chloride

The initiator synthesis was carried out in two steps in this system. The first step is the quaternization of amine group.

Figure 6.22. Initiator Synthesis Process for 6,1,10 (First Step)

1.5g 6-hydroxyhexan-1-amin (14.6 mmol) was dissolved in 20ml of DCM. Saturated Ether-HCl solution was added dropwise to previous solution. This mixed solution was stirred for 3h (according to our previous study, it was appeared that 3h stirring was enough to conversation from amine to ammonium) and the solvent was removed under *vacuo*. The yellowish product was separated.

The second step is the esterification of product 6-hydroxyhexan-1-aminium chloride with 2-bromo-isobutyryl bromide.

1.4 g of product 6-hydroxyhexan-1-aminium chloride (13.70 mmol) was dissolved in 10 ml anhydrous Acetone. The resulting solution was cooled in an ice bath and stirred for 2h. 2-bromoisobutyryl bromide (1.7 mL, 13.7 mmol) was dissolved in 5 ml anhydrous acetone. The solution was transferred to a dropping funnel. This 2-bromoisobutyryl bromide solution was dropwise added in 3h. After stirring the mixture for 20 h, the solvent and other impurities were evaporated. The final product was dissolved again in Acetone and precipitated in Diethylether. This molecule was isolated with 71% yield.

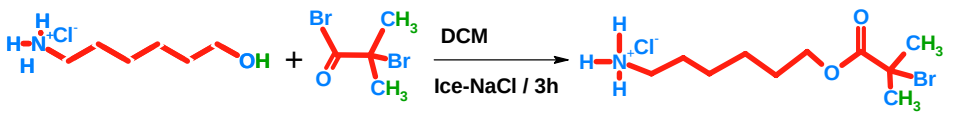

6-[(2-bromo-2-methylpropanoyl)oxy]hexan-1-aminium chloride

Figure 6.23. Initiator Synthesis Process for 6,1,10 (Second Step)

FTIR, ^{1}H NMR and ^{13}C NMR were used for characterization of the initiator which has been synthesized in two steps.

FTIR and NMR (^{1}H and ^{13}C) spectra were used for the identification of the structure 6-[(2-bromo-2-methylpropanoyl) oxy]

hexan-1-aminium chloride and showed the appearance of new peaks. The carbonyl peak is the most important among the others. This peak is observed at 1730 cm^{-1} as shown in figure 6.25. Another indicator of the structure 6-[(2-bromo-2-methylpropanoyl)oxy]hexan-1-aminium chloride is the $(CH_3)_2$ peak appearing at 1.85 ppm in ^{1}H-NMR, and the (RCOOR) peak at 171. 9 ppm in ^{13}C NMR. The related diagrams were shown in figure 6.26-6.28.

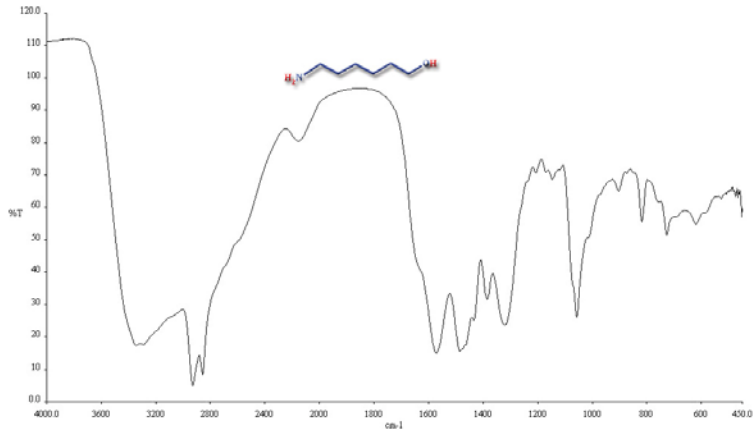

Figure 6,24. FT-IR spectrum of the 6-hydroxyhexan-1-amin

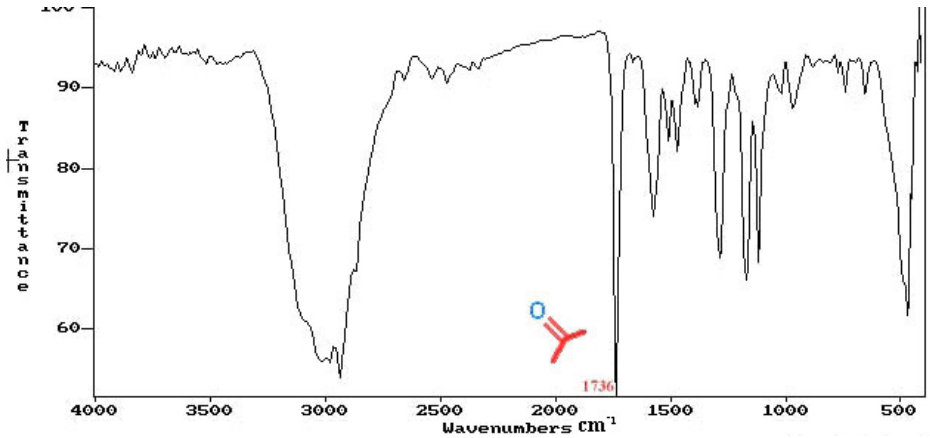

Figure 6.25. FT-IR Spectrum of the Structure 6-[(2-bromo-2-methylpropanoyl) oxy] hexan-1-aminium chloride

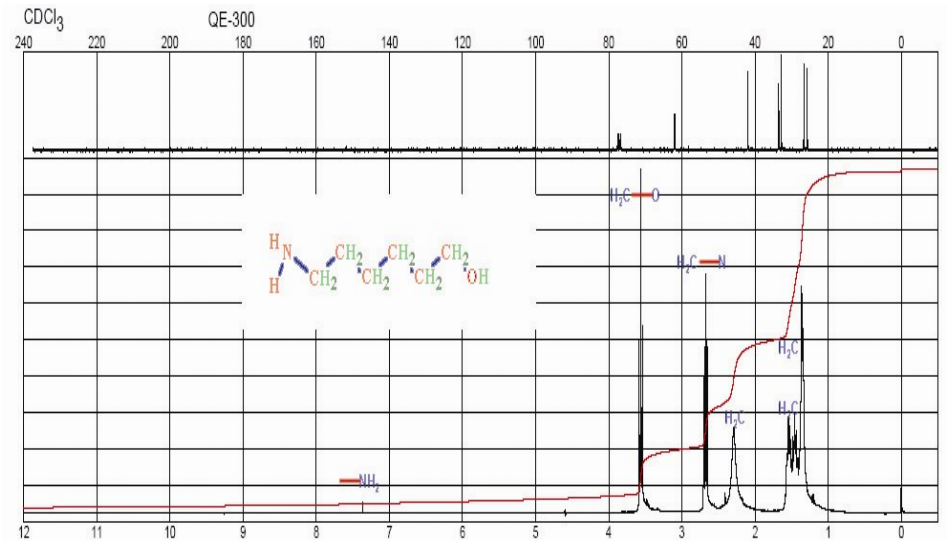

Figure 6.26. [1]H NMR Spectrum Of The 6-hydroxyhexan-1-amin

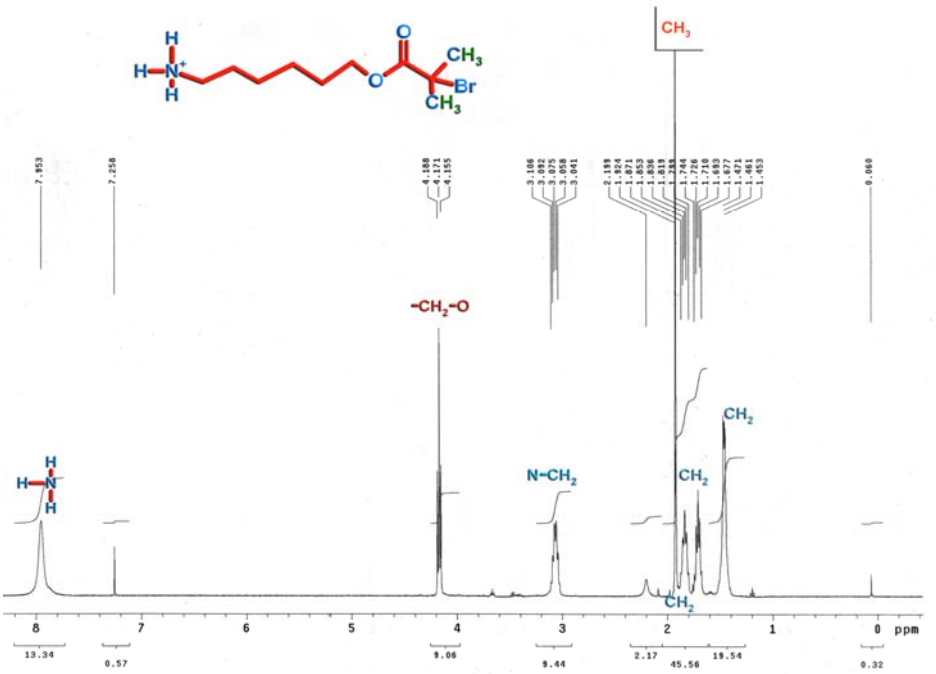

Figure 6.27. [1]H NMR Spectrum Of The Structure 6-[(2-bromo-2-methylpropanoyl) oxy] hexan-1-aminium chloride

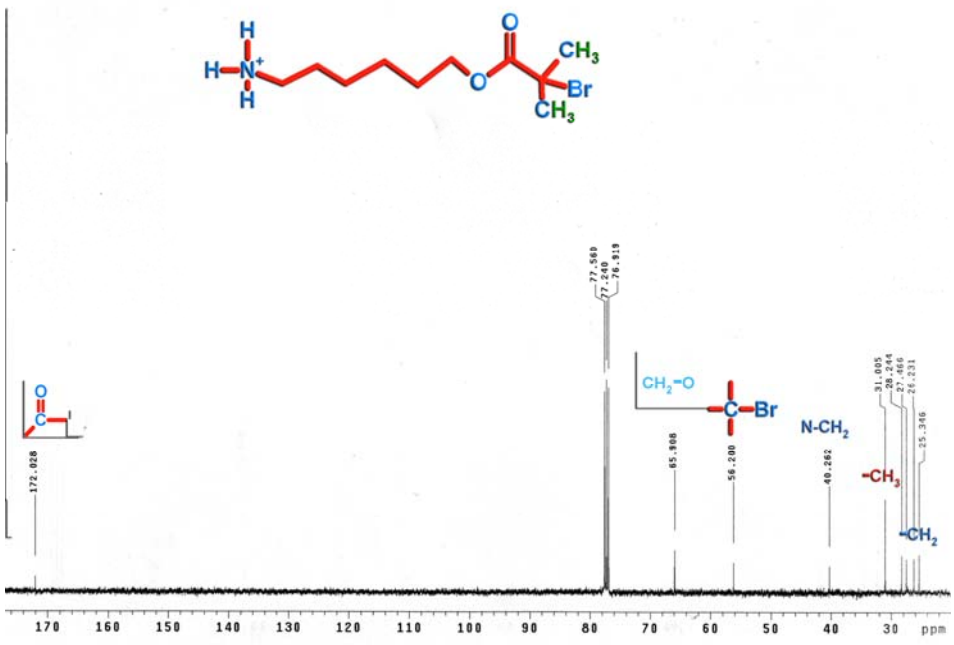

Figure 6.28. ^{13}CNMR Spectrum Of The 6-[(2-bromo-2-methylpropanoyl)oxy] hexan-1-aminium chloride

All of the data about the initiator were represented as below.

^{1}H NMR ($CDCl_3$, 300 MHz) 7.953 [s, 3H, NH_3], d 4.17 (t, 2H, CH_2O), 3.075 (m, 2H, CH_2N), 1.79 [s, 6H, $(CH_3)_2$], 1.744 (m, 2H, CH2), 1.726 (quintet, 2H, CH_2), 1.677 [m, 4H, $(CH_2)_2$]; ^{13}C NMR (300 MHz) d 171.59 (RCOOR), 64.98 (CH_2O), 52.01 [$(CH_3)_2CBr$], 40.47 [N-CH_2], 30.50 [(CH3)2], 28.25, 26.68, 25.18, 19.66, (CH2); FT-IR 3010, 2924, 2852, 1736, 1630,1503,1469, 1370, 1369, 1280, 1160, 1110, cm^{-1}.

6.2. Modification of Montmorillonite with Initiator and Characterization

Modification of the clay was done according to literature (Zhao[b] et al., 2003). Firstly the optimum ion exchange time was investigated. For this purpose 0.3 g of CTAB was dissolved in 20 ml of acetone. Five mixtures were prepared in the same way and composition. After these mixtures were stirred for 2h, 6h, 12h, 24h and 48h they were filtered and washed with acetone twice. The amount of immobilized CTAB was investigated via TGA: and for the time periods of 2h, 6h, 12h and 48h. The corresponding volatile materials are % 27.579, % 27.310, % 27.61 and % 27.535, respectively. The CEC value did not change versus time. For that reason the optimum CEC time for our study was the same as that in literature (Zhao[b] et al., 2003) and cation exchange process was done according to this literate.

The initiator was ion-exchanged onto montmorillonite. 1.0 g of montmorillonite was dispersed into acetone (50 mL) at room temperature. The dispersion was stirred for 30 min. 0.3 g initiator was added into the montmorillonite–acetone dispersion under vigorous stirring, which continued for 4 h. The mixture was then left without stirring for additional 12 h. The exchanged clay was filtered and washed with acetone twice. It was finally dried in vacuum at room temperature (Böttcher et al., 2002). The amount of immobilized initiator was determined by TGA as 63 mequiv immobilized initiator per 100g montmorillonite.

The modification step of montmorillonite (K10) with 6-[(2-bromo-2-methylpropanoyl)oxy] hexan-1-aminium chloride the is drawn in Figure 6.29 as below.

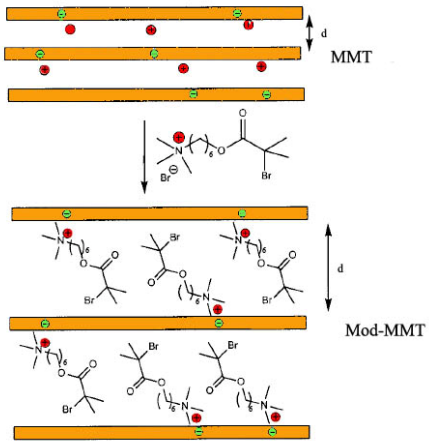

Figure 6.29. Modification Of The MMT (K10) With Product 6-[(2-bromo-2-methylpropanoyl) oxy]hexan-1-aminium chloride

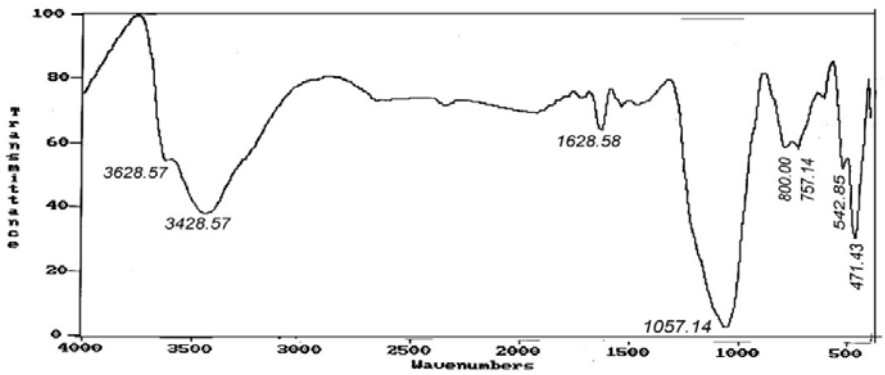

Figure 6.30. FT-IR Spectrum of the MMT (K10)

Montmorillonite shows a typically broad OH stretching band at 3622 cm^{-1}. Absorption bands of adsorbed molecular water are appearing at 1630 and 3400 cm^{-1}. They show a broadly similar pattern of adsorption at the 1150 cm^{-1} arising from Si-O stretching vibrations. More characteristic, however, are the well-resolved OH deformation bands at 915 cm^{-1} (Wilson, 1987). The absorption bands in the region below 550 cm^{-1} arise from Si-O stretching vibrations (Grim, 1968).

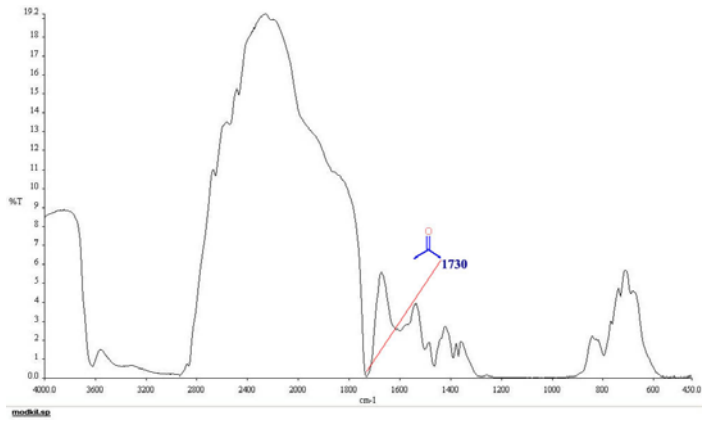

Figure 6.31. FT-IR Spectrum of the Modified MMT (K10)

Modified Montmorillonite was identified via FT-IR, TGA and XRD. If FT-IR spectrum of the pristine montmorillonite is compared with modified montmorillonite, a new carbonyl peak can be easily seen at 1730 cm^{-1} as shown in figure 6.31. This is a clear proof of the initiator modified MMT (K10).

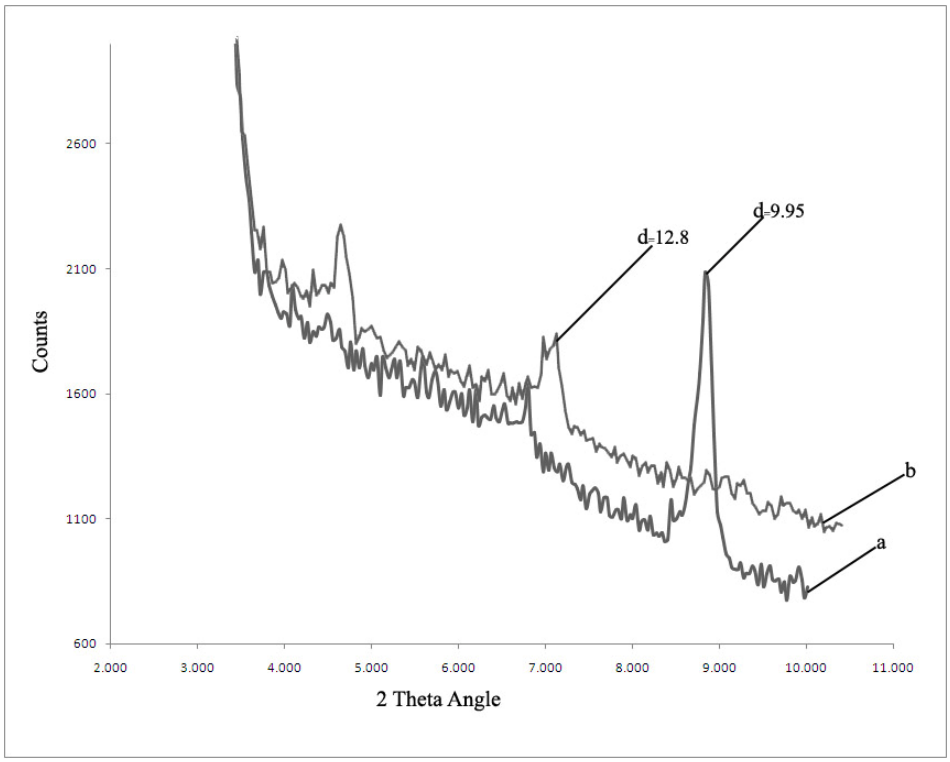

Figure 6.32. Plot Of X-Ray Diffraction (In Arbitrary Units) Versus Scattering Angle (In Degrees): (a) Montmorillonite (K10); (b) Initiator-Modified Montmorillonite.

Figure 6.32 displays a representative X-ray diffraction pattern. After ion exchange of clay with ATRP initiator, the interlayer distance increases from d_{001}~9.95 Å for the unmodified montmorillonite (a) to finally d_{001} ~ 12.8 Å (b). This is another indication of the formation of the initiator-modified montmorillonite, as a result of initiator penetration into interlayer of the montmorillonite leading to increasing interlayer spacing the clay.

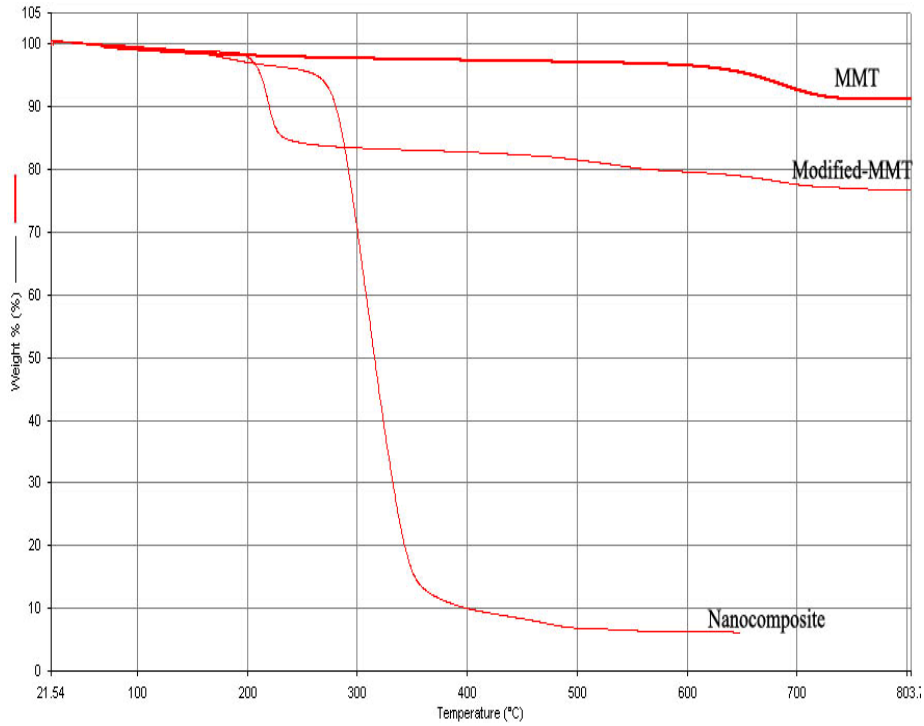

Figure 6.33. TGA Thermograms Of Unmodified MMT (K10) Modified MMT And Nanocomposite

According to TGA diagrams in figure 6.33, unmodified MMT (K10) was found to have 8.53wt % volatile materials. Thermogravimetric analysis (TGA) of modified montmorillonite reveals a silicate content of 22.8% which corresponds to 63 mequiv immobilized initiator per 100g silicate. This value is lower than for the case of complete ion exchange because according to (Yamaoka et al. 2000), the CEC capacity of the K10 is 1 mequiv/g. (Grim, R. E., 1968) and (Ray and Okamoto, 2003) argue that CEC values range from 60-120 mequiv/100g for smectic clays. (Ray and Okamoto, 2003) argue that CEC value 110 mequiv/100g for montmorillonite. When our value is compared with these values, it is seen that our value is smaller than the previously reported values. This is

attributed to the greater sterical demands of initiator than for small inorganic ions.

6.3. Nanocomposite Synthesis and Characterization

6.3.1. pHEMA Synthesis With Dibenzoylperoxide

After the 3,0 mL of HEMA was dissolved in 15 mL of solvent (70/30 v/v MEK/1-propanol), 0,024g of dibenzoylperoxide was added to this solution. This solution was stirred at room temperature for a 0,5h. Temperature was increased from room temperature to 80^0C and stirred for 2h. Product was precipitated in ether two times.

6.3.2. pHEMA Synthesis Via ATRP

The polymerization process was carried out according to literature (Beers et al., 1999). In a typical polymerization process all reactions were reported in previous polymerization process. It was only initiator (6-[(2-bromo-2-methylpropanoyl)oxy]hexan-1-aminium chloride) used instead of modified montmorillonite.

6.4. pHEMA-MMT (K10) Nanocomposite Synthesis

The polymerization process was carried out according to literature (Beers et al., 1999). In a typical polymerization process all reactions were

carried out in schlenk flasks equipped with a magnetic stirring bar. Firstly a 10 mL Schlenk flask was charged with 0.521 g modified montmorillonite (0.12 mmol initiator including). The flask was capped with a rubber septum and the contents were degassed by applying a vacuum and back-filling with argon three times. Modified montmorillonite and HEMA (3.0 mL; 25 mmol) which had been degassed with bubbling argon for at least 45 min were added by syringe and placed in a thermostated oil bath. The suspension was stirred for 30 min. In another 10 mL round-bottom flask 0.0172 g (0.12 mmol) of CuBr and 0.0386 g of Bpy (0.241 mmol) were degassed by vacuum followed by argon backfill three times. The solvent (70/30 v/v MEK/1-propanol; 3.0 mL) was added via syringe. This solution (transition metal catalyst complex) was transferred from this Schlenk into another Schlenk via cannula. The reaction mixture was stirred in a 55 ^{0}C oil bath for 1 h under nitrogen. The polymergrafted montmorillonite was precipitated in diethylether. Finaly the nanocomposite was collected and dried under *vacuum*.

The structure of the nanocomposite was characterized via ^{1}HNMR, ^{13}CNMR, and XRD and its properties were investigated using TGA, DSC, TEM, and GPC, techniques. In the study nanocomposite was synthesized by in situ polymerization method via ATRP. The mechanism of ATRP is presented in figure 6.34.

Because the initiator was intercalated into galeries of the montmorillonite, these reactions occurred in these sites. As a result of these reactions the d spaces of the montmorillonite increases.

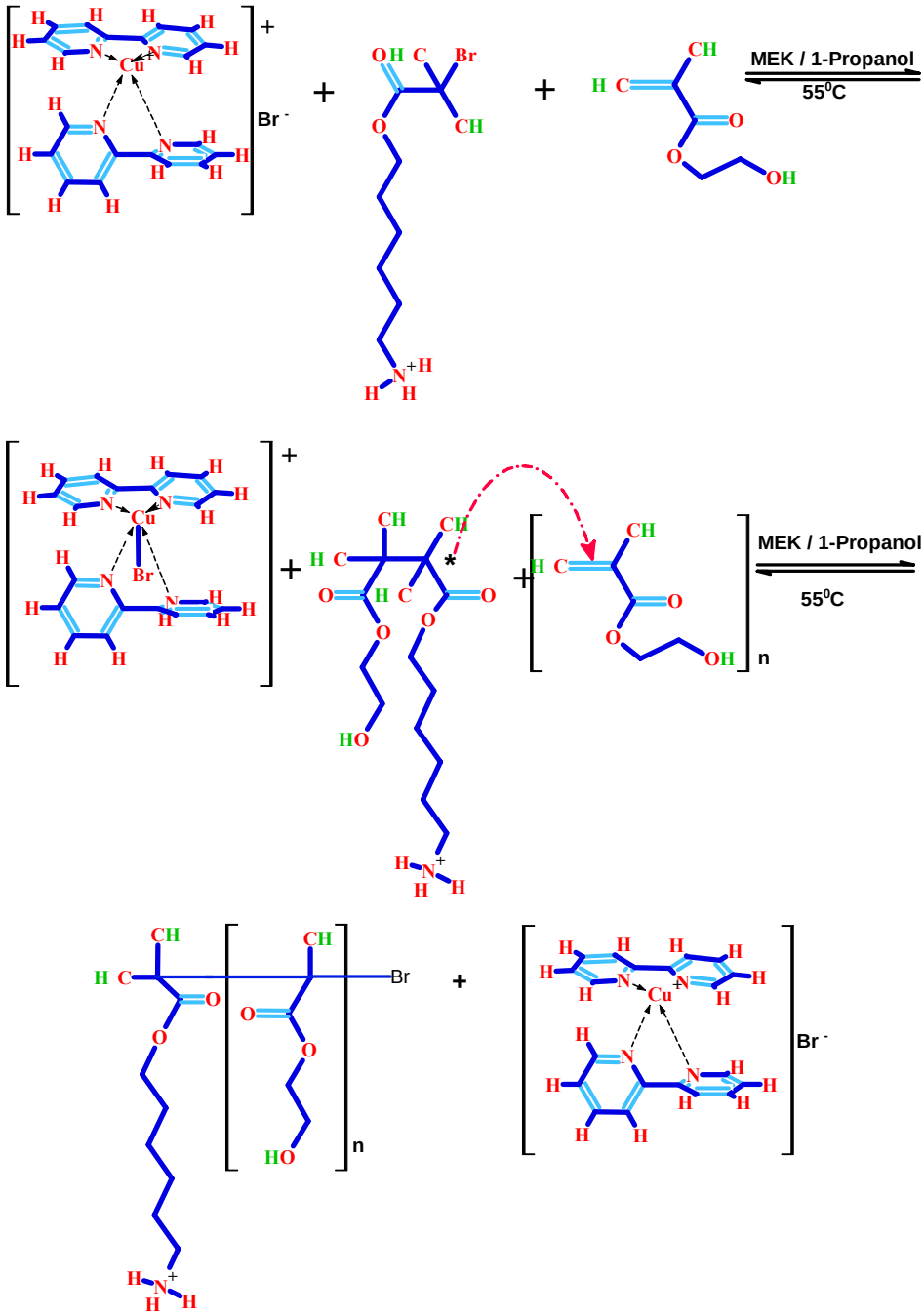

Figure 6.34.. Polymerization Mechanism copper(I) Halide, Bidentate Ligand (bpy) and HEMA

ATRP process depends on redox potential and halogenophilicity of the transition metal complex. After the oxidation from Cu^{I} to Cu^{II} ,Cu^{II} complex is formed. The reaction is initiated by the activation (homolytic cleavage) of the carbon-halogen bond in alkylammonium initiator (R-X) via one-electron oxidation of the metal center (M^n X^nL) to form an initiating radical species (R^*) and the active transition metal complex that trigonal bipyramidal cationic structure $[X\text{-}Cu(II)(bpy)_2]^+$ generates. The R^* adds to the monomer to generate a radial species (monomeric radical). Polymer chains grow by the addition of the intermediate radicals to monomers in a manner similar to a conventional radical polymerization (Giannelis, 1998).

Although the d_{001} diffraction peak in the XRD pattern of modified montmorillonite has finally disappeared, the layered structure is retained to a certain extent. After the polymerization, the silicate layers were completely delaminated as evidenced by the absence of any diffraction peak. The d_{001} diffraction peak of the polymer/clay nanocomposite disappeared, potentially indicating that much of the layered structure in the clay particles was destroyed by polymerization. However, a caveat is that, the low clay content and low 2θ values limit XRD analysis in terms of providing definitive proof or quantitative measurement of exfoliation (Zhaoa and Shipp, 2003).

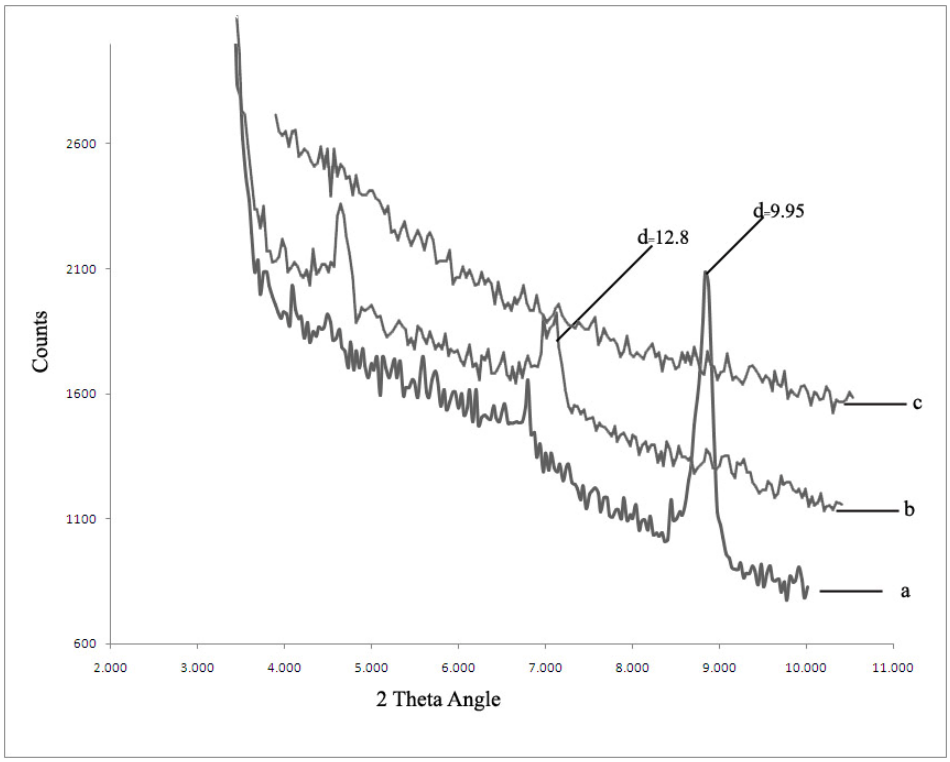

Figure 6.35. X-ray Diffraction Diagram Of MMT (K10), Modified MMT (K10) And PHEMA/Clay Nanocomposite (a) Montmorillonite K10; (b) Initiator-Modified Montmorillonite (K10); (c) PHEMA/Clay Nanocomposite.

Figure 6.35 shows the XRD diagrams of the clay, ATRP initiator modified clay and pHEMA/clay nanocomposite. For the pHEMA/clay nanocomposite, the 001 diffraction peak on XRD spectra disappeared, which implies that the layered structure in the clay particles is largely destroyed by in situ polymerization. However, because of the low content of clay in the nanocomposite, XRD analysis is not accurate enough to characterize the type of composites.

These XRD results agree with literate (Zanetti et al., 2000).

TEM micrographs are shown in figure 6.36. It was observed from these images that exfoliated, intercalated and stacked montmorillonite platelets were present in the matrix. Exfoliated, intercalated and stacked platelets (microcomposite) are represented respectively as (a), (b) and (c). Nanocomposite system seems to certain both exfoliated and intercalated structures rather than only exfoliated structures. From the images, it could be seen that some clay-rich sites were created in the nanocomposites matrixes. Montmorillonite K10 which was acid treated has attractive sites on its surfaces and edges, and the polymer has too. As a consequence of this strong interaction between MMT (K10) and pHEMA occurs and polymer chains can not penetrate totally into intergaleries of the MMT (K10). Thus, ideal mixing of polymer chains with MMT could not be done.

Another affect is lower CEC of the MMT (K10). As a result of lower initiator penetration into interlayer of the montmorillonite, leading to lower numerous initiators and lower numerous polymer backbones. The other parts of the MMT are not affected in polymerization progress.

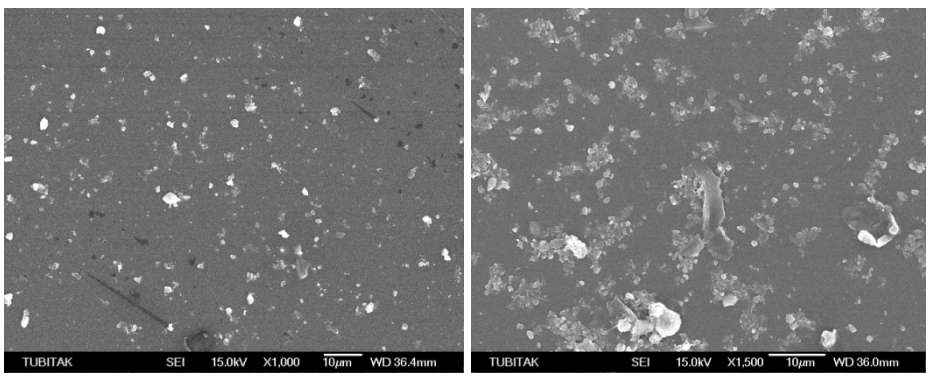

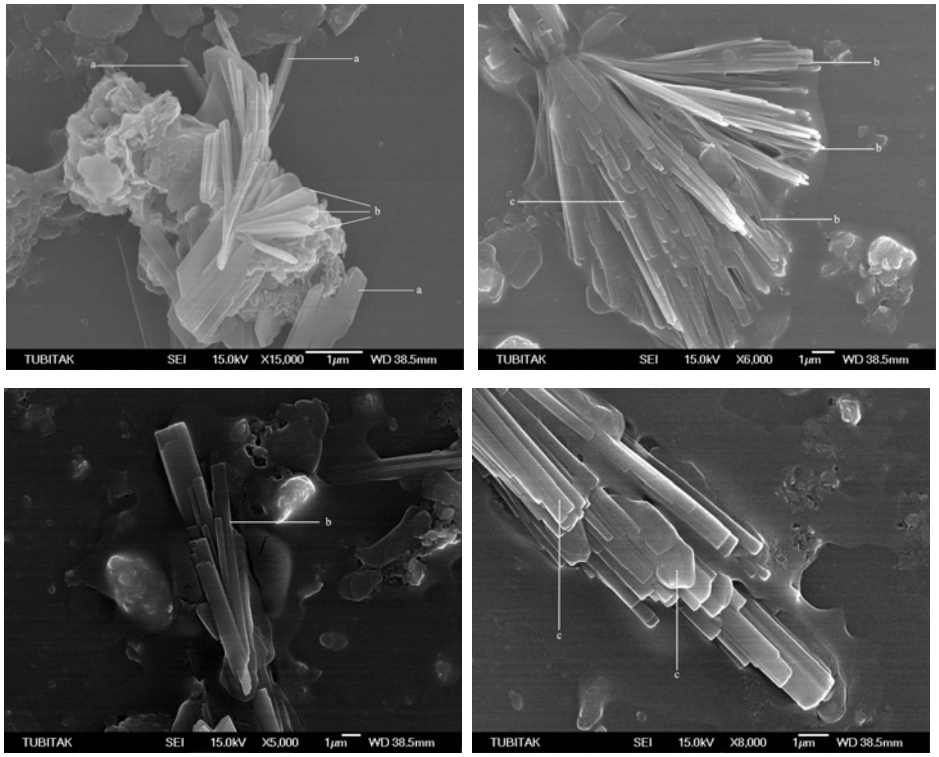

Figure 6.36. TEM micrographs Of Phema–Montmorillonite Nanocomposite With Various Magnification

Molecular weights were measured by gel permeation chromatography. In the first place the nanocomposite has to be purified. This purification was done in two steps: in the first step; the nanocomposite (100 mg) was suspended in MEK/1-propanol (150 mL). 20 mg sample of p-Toluenesulfonic acid was added and the mixture was heated under reflux for 14 h. The mixture was transferred to centrifuge tubes and the solid material was separated by centrifugation. The supernatant was separated by decantation and the solution was passed through a column of alumina. The solution was concentrated in *vacuo*

and the polymer was precipitated in Ether. Finally the polymer was filtered off and dried at 50 ^{0}C and 10 mbar to constant weight.

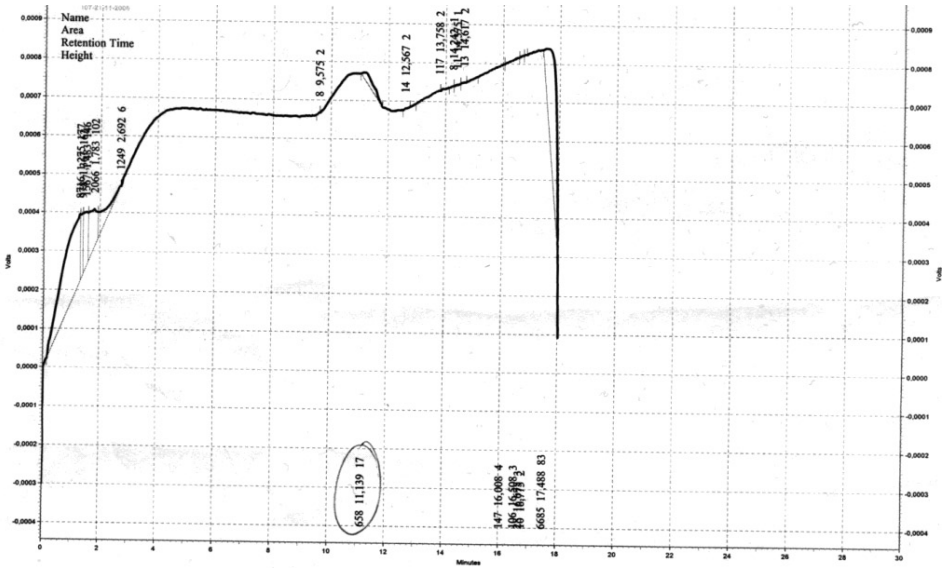

Figure6.37. GPC Traces of Phema (Extracted Montmorillonite Nanocomposites)

According to GPC traces in figure 6.37, M_n=276778, M_w= 282579 and M_w/M_n=1.021 results were obtained. These results mean that narrow molecular weight distribution was achieved.

Polymer chains mobility is important in the nanocomposite because of the effect on the thermal properties. Greater mobility may be due to an ordering that occurs between the layers, which creates low- and high-density regions, thus providing the opportunity for mobility in the low-density regions. If the polymer is tethered to the clay, the clay can reduce the mobility locally. The glass transition temperature can be eliminated for clay nanocomposites with intercalated polymer chains. This indicates

a limited ability for cooperative chain motion when the polymers are confined between the layers. If the clays are exfoliated, and thus the polymer is not confined between layers, the T_g does not change significantly (Ajayan et al, 2003).

T_g increases for strong polymer/filler interactions and decreases for weak interactions (Becker et al., 1998).

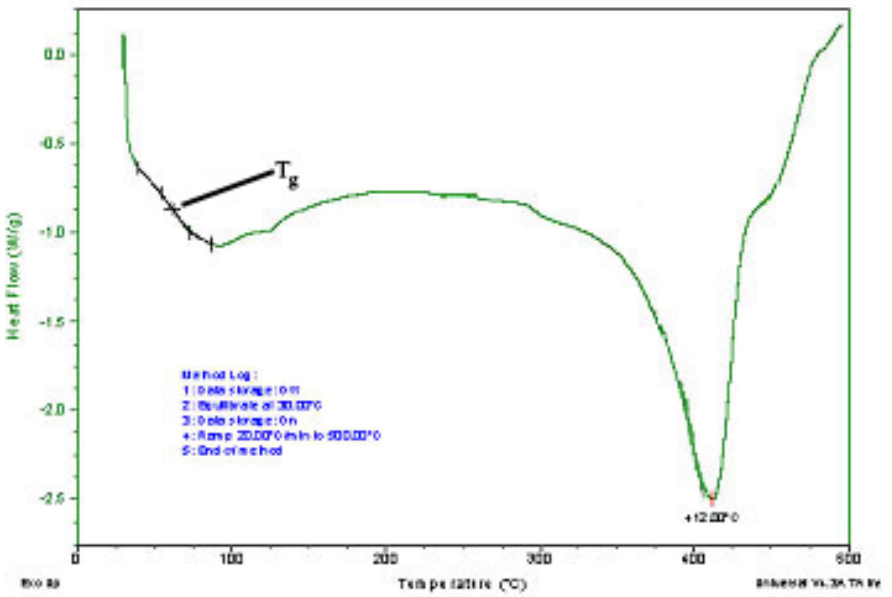

Figure 6.38. DSC Thermograms Of Pure pHEMA(ATRP)

According to DSC diagrams; Tg temperature of the nanocomposite decreased slightly. Tg of the pure pHEMA (synthesized via ATRP) is 60.98 ^{0}C and Tg of the nanocomposite is 55.12 ^{0}C, i.e. Tg decreased by 5.86 ^{0}C. High density regions might be formed because of some

intercalating and stacking structures in the matrix. Stacking areas causes a decrease in Tg if polymer clay interaction is weak. Intercalating structures tend to increase the Tg value if polymer clay interaction is strong. In case of exfoliated structure, Tg does not change significantly. Moreover, molecular weight of the polymer (Mn), particle size, quantity of crosslink in polymer, surface area and polarity of polymer and filler affect Tg. All of the parameters affect polymer clay interaction, mobility and segmental motion of the polymer backbones. Intercalated, exfoliated and microcomposite structures in the polymer matrix are consequence of this, changing of Tg is rather small quantity than expected in only one type nanocomposite. Finally, Tg decreased and consuming energy for polymer processing such as molding, extruding declined as a result of this decrease.

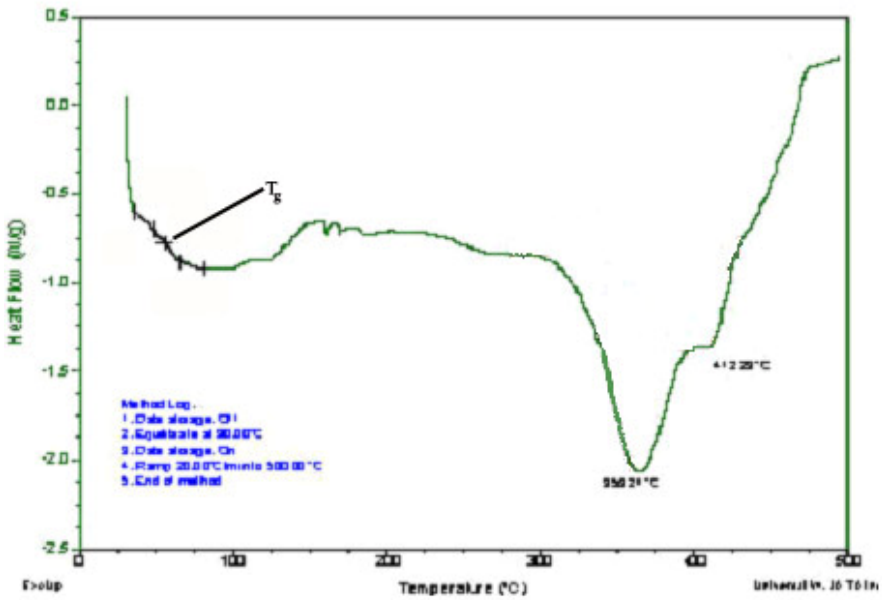

Figure 6.39. DSC Thermograms Of pHEMA-Nanocomposite

The thermal stability of a material is usually assessed by thermogravimetric analysis (TGA) where the sample mass loss due to volatilization of degraded by-products is monitored as a function of a temperature ramp.

Thermal parameters are related to both particle size of the inorganic filler and mobility of the polymer chains in the matrix. The sizes of the fillers lead to an exceptionally large effect on interfacial area in the composite. The interfacial region is extremely large in nanocomposites. The polymer–particle interaction is occurred in this area. The interaction of the polymer with the nanoparticles gives significant opportunity for changing the polymer mobility and relaxation dynamics. Small size means that the particles do not create large stress concentrations and thus do not compromise the ductility of the polymer. The small size of nanofillers can also lead to unique properties of the particles themselves.

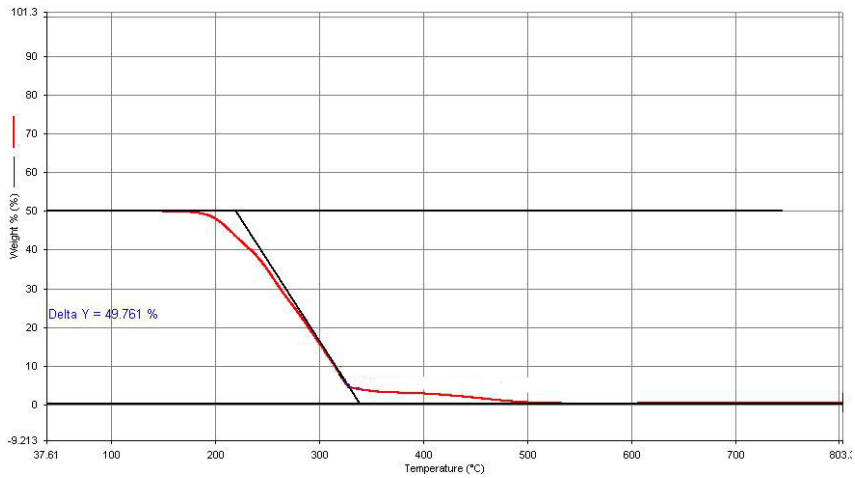

Figure 6.40. TGA Thermogram Of 6-[(2-Bromo-2-Methylpropanoyl)Oxy] Hexan-1-Aminium Chloride (15^0C/min, in air)

As seen in figure 6.40, synthesized initiator is completely decomposed at relatively low temperatures. This initiator has rather a small quantity (% 0.48) in the matrix. For that reason its own decomposition peak can not be seen in pure pHEMA and nanocomposite process.

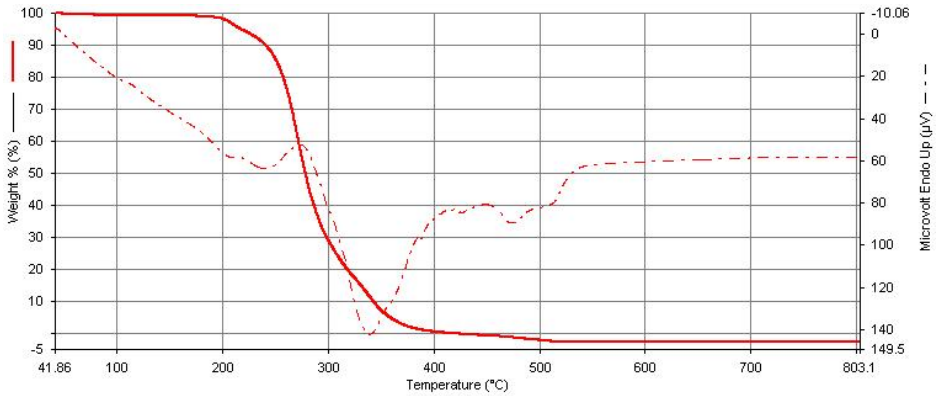

Figure 6.41. TGA-DTA Thermogram of pHEMA(BzO_2), (15^0C/min, in air)

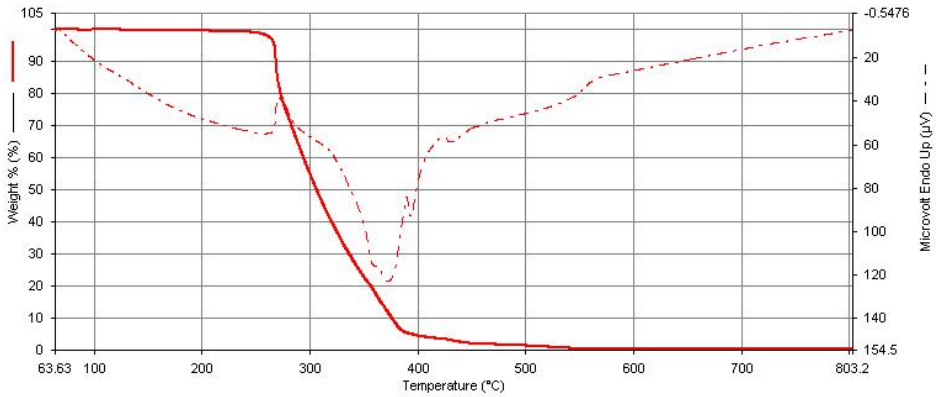

Figure 6.42. TGA-DTA Thermogram of pHEMA (ATRP), (15^0C/min, in air)

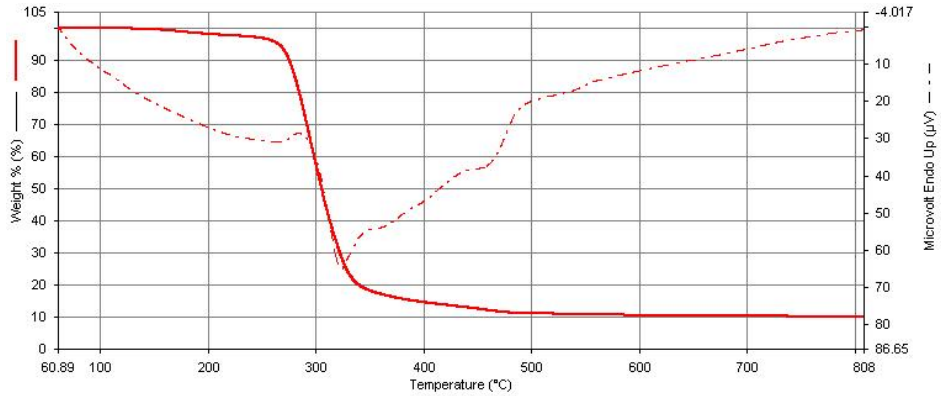

Figure 6.43. TGA-DTA Thermogram of pHEMA-Nanocomposite (15^0C/mim, in air)

pHEMA is known to decompose in two consecutive steps. Overall decomposition process consists of two kinds of reactions: one of them is depolymerization to the monomer, which is the major reaction low temperature decomposition. The other various decomposition reactions on the ester side chain, which occurs at high temperatures (Demirelli et al. 2001). In our studies thermogravimetric analysis (TGA) reveals that the inflection point of the nanocomposite in air is 45.9 ^{0}C higher than pHEMA. Maximum temperatures of thermal degradation (inflection point) of the pHEMA (synthesized with the BzO_2), pure pHEMA (synthesized via ATRP) and nanocomposite are respectively 274.2 ^{0}C, 268.74 ^{0}C and 314.65 ^{0}C in air. If similar investigation is done under N_2 atmosphere, the inflection point of the pHEMA (synthesized with the BzO_2), pure pHEMA (synthesized via ATRP) and nanocomposite are respectively 405.6 ^{0}C, 400.95 ^{0}C and 408.75 ^{0}C.

Table 6.1. Degradation Energies of pHEMA-Nanocomposite, pHEMA(ATRP) and pHEMA(BzO_2),

Material	In Air		In Nitrogen	
ΔH (J/g)	ΔH_1	ΔH_2	ΔH_1	ΔH_2
pHEMA (BzO_2)	56.7	-2148.5	23.3	-117.2
pHEMA (ATRP)	40.8	-2504.7	160.6	-127.0
pHEMA-MMT Nanocomposite	23.2	-1580.4	280.7	-7.04

Two decomposition energies are shown in Table 6.1. Degradation energies of pHEMA(ATRP) compared with pHEMA-MMT (K10) nanocomposite in air medium, ΔH_1 decreased 17.6 J/g (endothermic) and ΔH_2 decreased 924,3 J/g (exothermic). In nitrogen, the pHEMA-MMT nanocomposites have a 120.1 J/g (endothermic) increasing and 120.0 J/g (exothermic) decreasing were seen. Nanocomposite exhibits a rather large increase in thermal stability as a result of the increase in the endothermic energies and decrease in the exothermic energies or small changes in endothermic energies.

The activation energy of degradation according to Ozawa Method (Ozawa, 1965) for pHEMA (ATRP) in air is 510.715 J/mol. Activation energy of degradation according to Ozawa Method for pHEMA-MMT (K10) nanocomposite in air is 16453.2 J/mol.

These results mean that, the nanocomposite is more stable than the pure polymer. The stability of the pHEMA nanocomposite is commonly due not only to its different structure but also to restricted thermal motion of the pHEMA molecules in the gallery.

In oxidative decomposition, the explanation for the improved thermal stability is char formation occurring under oxidative conditions. The char act a physical barrier between the polymer and superficial zone where the combustion of the polymer is running (Beyer, G., 2002). Other effects include heat barrier effect of the clays in the matrix and declining gas diffusion properties because of the clay stacks. In oxidative degradation, if oxygen cannot penetrate, then it cannot cause oxidation of the polymer. Moreover, silicates are also known for their excellent thermo-oxidative stability to provide a retarding effect on the thermal degradation of the organic component of the nanocomposites. Therefore, the MMT (K10) should also enhance heat resistance of the phenolic resins of the nanocomposites. These are the explanation for the improved thermal stability of the pHEMA-MMT (K10) nanocomposite.

The explanation for the non-oxidative decomposition is similar to oxidative. The clay acts as a heat barrier, which enhances the overall thermal stability of the system, as well as assist in the formation of char after thermal decomposition. In the early stages of thermal decomposition, the clay would shift the decomposition to higher temperature. After that, this heat barrier effect would result in a reverse thermal stability. In other words, the stacked silicate layers could hold

accumulated heat that could be used as a heat source to accelerate the decomposition process, in conjunction with the heat flow supplied by the outside heat source ([b]Ray and Okamoto, 2003). Gas diffusion is not so important that oxidative case. For that reason, the change in thermal stability is smaller than oxidative state.

Our studies thermogravimetric analysis (TGA) reveals that the inflection point of the nanocomposite in air is 45.9 ^{0}C, higher than pHEMA. These results agree with the results of ([b]Ray and Okamoto, 2003) and (Alexandre and Dubois, 2000). They were found out that intercalated PMMA-MMT nanocomposites have 40 – 50 ^{0}C higher decomposition temperature.

In both cases (air, nitrogen) Na-montmorillonite (microcomposite) does not influence the thermal degradation of the matrix (Alexandre et al., 2000). Namelly, the stability of the Na-montmorillonite (microcomposite) does not change compared with pure polymer. The thermal stability of the modified clay composite is increased. If the microcomposite structure is more quantity than the others in our studies, thermal stability of the polymer-MMT composite is not increased. But, the thermal stability of the polymer-MMT (K10) composite increased for our study.

The dispersion of the clays is critical to increasing the degradation temperature. Delaminated composites have significantly higher degradation temperatures than intercalated nanocomposites or traditional

clay composites (Lee et al., 1997). Thermal stability of the polymer-MMT composite does not increase as high as exfoliated. This is meant that exfoliated structure is not more quantity than the others,

These results clearly indicate that intercalated structure in the polymer matrix is quite larger in quantity than exfoliated structure. This is verifying that the majority of the structures are intercalated.

7. CONCLUSIONS

First of all, the initiator consisting of quaternary ammonium salt moiety and an ATRP initiator moiety was designed and synthesized. This initiator was then penetrated to intergaleries of the MMT thus MMT was modified.

Polymerization of HEMA was carried out by in situ ATRP with this modified MMT system thus synthesis of polymer-clay nanocomposite which had predictable properties such as thermal and physical properties of polymer by the addition of modified MMT was achieved. Polymerization reaction of HEMA was carried out in a mixed solvent system consisting of methyl ethyl ketone and 1-propanol at 55 ^{0}C, used the 6-[(2-bromo-2-methylpropanoyl) oxy] hexan-1-aminium chloride that has been already synthesized with a copper (I) bromide catalyst. The 2, 2'-bipyridyl (bpy) complex was used as ligand.

As a consequence of the some GPC, DSC and TGA diagrams and traces, molecular weight of the pHEMA was M_n=276778 and M_w/M_n=1.021, increase in the thermal degradation temperature of polymer was 45.9 ^{0}C in air, 7.8 ^{0}C in N_2 and decrease of Tg about 5.86 ^{0}C were observed. Degradation energies of pHEMA(ATRP) compared with pHEMA-MMT nanocomposite for air medium, ΔH_1 decreased 17.68 J/g (endothermic) and ΔH_2 decreased 924,3 J/g (exothermic). In nitrogen the pHEMA-MMT nanocomposites have a 120.15 J/g (endothermic) increasing and 120.03 J/g (exothermic)

decreasing were calculated. Activation energy of degradation according to Ozawa Method (Ozawa, 1965) for pHEMA (ATRP) in air is 510.715 J/mol. Activation energy of degradation according to Ozawa Method for pHEMA-MMT nanocomposite in air is 16453.2 J/mol, i.e. the thermal degradation temperature has increased.

TEM analysis and XRD results showed the existence of microcomposite, intercalated and exfoliated structures in the pHEMA-nanocomposite matrix but as supported by TGA and DSC analysis, the majority of the structures in the matrix are intercalated.

REFERENCES

Ajayan, P. M., Schadler, L. S., Braun, P. V., 2003,*Nanocomposite Science and Technology*, WILEY-VCH Verlag GmbH Co. KGaA, Weinheim, 96.

Alexandre, M., Dubois, P., 2000, Materials Science and Engineering, 28, P:55.

Amass, A. J., Wyres, C. A., Colclough, E., Hohn, I. M., 1999, *Polymer,41*, 1697.

Ando, T., Kamigaito, M., Sawamoto, M., 1997, *Macromolecules,* 30, 4507.

Ando, T., Kamigaito, M., Sawamoto, M., 1997, *Tetrahedron, 53*, 15445.

Ando, T., Kamigaito, M., Sawamoto, M., 2000, *Macromolecules,* 33, 5825.

Ando, T., Kato, M., Kamigaito, M., Sawamoto, M., 1996, *Macromolecules,* 29, 1070.

Aranda, P., Ruiz-Hitzky, E., 1992, Poly(ethylene oxide)-silicate intercalation materials, *Chem Mater*,4:1395–403.

Asayama, S., Akaike, T., Maruyama, A., 2001, Colloids and Surfaces B: Biointerfaces, 22, 183.

Bamford, C., Allen, G., Aggarwal, S. L., Russo, S., 1989, *Comprehensive Polymer Science*, Pergamon: Oxford, 3, 123.

Becker, C., Mueller, P., Schmidt, H., 1998, SPIE, 88, 3469.

Beers, K. L., Boo, S, Gaynor, S. G., and Matyjaszewski, K., 1999, *Macromolecules*, *32,* 5772-5776.

Bengough, W. I., Fairservice, W. H., 1971, *Trans. Faraday Soc.* 67, 414.

Beyer, G., 2002, Plastic Aditives & Compounding, p:26.

REFERENCES (Continued)

Bharadwaj, R. K., 2001, Modeling the barrier properties of polymerlayered silicate nanocomposites, *Macromolecules* 34,1989.

Biswas, M., Sinha Ray, S., 2001,Recent progress in synthesis and evaluation of polymer–montmorillonite nanocomposites, *Adv Polym Sci* 155,167.

Blasse, G., Dirksen, G. J., Brenchley, M. E., Weller, M. T., 1995, *Chem. Phys. Lett., 234*, 177.

Bourbigot, S., LeBras, M., Dabrowski, F., Gilman, J. W., Kashiwagi, T., 2000, PA-6 clay nanocomposite hybrid as char forming agent in intumescent formulations, *Fire Mater*, 24, 201–8.

Boutevin, B., 2000, *J. Polym. Sci., Part A: Polym. Chem., 38*, 3235.

Böttcher, H., Hallensleben, M. L., Nuß, S., Wurm, H., Bauer, J., Behrens, P., 2002, *Journal of Materials Chemistry*, 12, 1352.

Brandts, J. A. M., van de Geijn, P., van Faassen, E. E., Boersma, J., van Koten, G., 1999, *J. Organomet. Che., 584*, 246.

Brenchley, M. E., Weller, M. T., 1993, *Angew. Chem., 105*, 1726.

Brindly, S. W., Brown, G., 1980, Crystal structure of clay minerals and their X-ray diffraction., *MineralogicalSociety*.

Cassagneau, T., Hix, G. B., Jones, D. J., Maireles-Torres, P., Rhomari, M., Roziere., 1994, *J. Mater. Chem.*, *4*, 189.

Chen, X. Y., Parmes, S. P., Greaves, S. J., Watts, J. F., 2004, Langmuir, 20, 587.

Cheng, G. L., Hu, C. P., Ying, S. K., 1999, *J. Mol. Catal. A: Chem.* 144, 357.

Cheng, G. L., Hu, C. P., Ying, S. K., 1999, *Macromol. Rapid Commun.,* 20, 303.

Curran, D. P., 1988**,** *Synthesis*, 489.

REFERENCES (Continued)

Curran, D. P. In, Trost, B. M., Fleming, I., Eds., 1991, *Comprehensive Organic Synthesis*, Pergamon: Oxford, U.K., Vol. 4, pp 715-777. (b) Iqbal, J., Bhatia, B., Nayyar, N. K. Chem. R*ev*. **1994**, *94*, 519-554.

Dabrowski, F., Bras, M Le., Bourbigot, S., Gilman, J. W., Kashiwagi, T., 1999, PA-6 montmorillonite nanocomposite in intumescent fire retarded EVA, *Proceedings of the Euro-fillers'99*, Lyon-Villeurbanne, France, 6–9 September.

Dalton, P. D., Flynn, L., Shoichet, M. S., 2002, Manufacture of poly(2-hydroxyethyl methacrylate-co-methyl methacrylate) hydrogel tubes for use as nerve guidance channels, *Biomaterials,* 23, (18), 3843.

Davis, K., O'Malley, J., Paik, H. j., Matyjaszewski, K., 1997, *Polym. Prepr. (Am. Chem. Soc., Div. Polym. Chem., 38* (1), 687.

Davis, K., Paik, H.-j., Matyjaszewski, K., 1999, *Macromolecules 32*, 1767.

Del Rio, I., van Koten, G., Lutz, M., Spek, A. L., 2000, *Organometallics, 19*, 361.

Demirelli, K., Coşkun, M., Kaya, E., 2001, Polymer Degradation and Stability, 72, 75-80.

Destarac, M., Bessie`re, J. M., Boutevin, B., 1997, *Macromol. Rapid Commun., 18*, 967.

Flynn, L., Dalton, P. D., Shoichet, M. S., 2003, Fiber ternplating of poly(2-hydroxyethyl methacrylate) for neural tissue engineering. *Biomaterials,* 24, (23), 4265.

Giannelis E. P., 1996, Polymer layered silicate nanocomposites, *Adv Mater,* 8:29–35.

Giannelis, E. P., 1998, Polymer-layered silicate nanocomposites:

REFERENCES (Continued)

synthesis, properties and application, *Appl., Organomet., Chem.,* 12, 675–80.

Giannelis, E. P., Krishnamoorti, R., Manias, E., 1999, Polymer-silicate nanocomposites: model systems for confined polymers and polymer brushes, *Adv Polym Sci,* 138, 107–47.

Gilman, J.W., 1999, Flammability and thermal stability studies of polymer-layered silicate (clay) nanocomposites, *Appl. Clay Sci.,* 15,31–49.

Gilman, J.W., Jackson, C.L., Morgan, A.B., Harris, Jr R., Manias, E., Giannelis, E.P., Wuthenow, M., Hilton, D., Phillips, S.H., 2000, Flammability properties of polymer-layered silicate nanocomposites. Propylene and polystyrene nanocomposites, *Chem Mater*, 12, 1866–73.

Gilman, J.W., Kashiwagi, T., Lichtenhan, J.D., 1997, Flammability studies of polymer-layered silicate nanocomposites, SAMPE J., 33, 40–5.

Goto, A., Fukuda, T., 1999, *Macromol. Rapid Commun., 20*, 633.

Granel, C., Dubois, P., Je´roˆme, R., Teyssie´, P., 1996, *Macromolecules, 29*, 8576.

Greenland, D. J., 1963, Adsorption of poly(vinyl alcohols) by Montmorillonite, *J Colloid Sci ,*18, 647.

Grim, R. E., 1968, Clay Mineralogy, 2nd edit., p.362, McGraw Hill, New York, NY, USA.

Guo, J., Han, Z., Wu, P., 2000, *J. Mol. Catal. A: Chem., 159*, 77.

Hackett, E., Manias, E., Giannelis, E.P., 1998, Molecular dynamics simulations of organically modified layered silicates, *J. Chem. Phys.,* 108, 7410.

Haddleton, D. M., Jasieczek, C. B., Hannon, M. J., Shooter, A., 1997, *J. Macromolecules*, *30*, 2190.

REFERENCES (Continued)

Hay, M, P., Pruijn, F. B., Gamage, S, A., Liyanage, H. D. S., Kovacs, M.S., Patterson, A. V., Wilson, W. R., Brown, J. M., Denny, W. A., 2004, J. Med. Chem., 47, 475.

Henglein, A., Fojtik, A., Weller, H., 1987, *Ber. Bunsen-Ges., 91*, 441.

Heuts, J. P. A., Mallesch, R., Davis, T. P., 1999, *Macromol. Chem. Phys., 200*, 1380.

Ito, E., Suzuki, K., Yamato, M., Yokoyama, M., Sakurai, Y., Okano, T., 1998, Active platelet movements on hydrophobic/hydrophilic microdomain-structured surfaces., *Journal of Biomedical Materials Research,* 42, (1), 148-155.

Jeon, H. G., Jung, H., and Hudson, S. D., 1998, Morphology of polymer/silicate nanocomposites, *Polymer Bulletin*, **41**, 107-113.

Kato, M., Kamigaito, M., Sawamoto, M., Higashimura, T., 1995, *Macromolecules, 28*, 1721.

Kawasumi, M., Hasegawa, N., Usuki, A., and Akane, O., 1998, Nematic liquid crystal/clay mineralcomposites, *Mater. Eng. Sci. C*, **6**, 135-143.

Khan, A. J., Percival, S. P. B., 1999, 12 year results of a prospective trial comparing poly(methyl methacrylate) and poly(hydroxyethyl methacrylate) intraocular lenses., *Journal of Cataract and Refractive Surgery,* 25, (10), 1404.

Kharasch, M. S., Jensen, E. V., W. H., U., 1945, *Science, 102*, 128.

Kickelbick, G., Matyjaszewski, K., **1999**, *Macromol. Rapid Commun., 20*, 341.

Klein, D. L., Roth, R., Lim, A. K. L., Alivisatos, A. P., McEuen, P. L., 1997, *Nature, 389*, 699.

Kofoed, T., Henrik, F. H., Ørum, H., Koch, T., 2001, *Journal of Peptide Science, 7*, 402.

REFERENCES (Continued)

Kojima, Y., Usuki, A., Kawasumi, M., Fukushima, Y., Okada, A., Kurauchi, T., Kamigaito, O., 1993, Mechanical properties of nylon 6–clay hybrid., *J Mater Res.,* 8, 1179–84.

Kotani, Y., Kamigaito, M., Sawamoto, M., 1999, *Macromolecules, 32*, 2420.

Kotani, Y., Kato, M., Kamigaito, M., Sawamoto, M., 1996, *Macromolecules, 29*, 6979.

Krishnamoorti, V., R., Giannelis, E., P., 1996, Structure and dynamics of polymer-layered silicate nanocomposites., *Chem Mater*, 8, 1728–34.

Lagaly, G., 1986, Interaction of alkylamines with different types of layered compounds., *Solid State Ionics,* 22, 43–51.

Laus, M., Camerani, M., Lelli, M., Sparnacci, K., Sandrolini, F., and Francescangeli, O., 1998, Hybrid nanocomposites based on polystyrene and a reactive organophilic clay, *J. Mater. Sci*., **33**, 2883-2888.

LeBaron, P. C., Wang, Z., Pinnavaia, T., J., 1999, Polymer-layered silicate nanocomposites: an overview, *Appl Clay Sci.,* 15, 11–29.

Leclere, P., Moineau, G., Minet, M., Dubois, P., Jerome, R., Bredas, J. L., Lazzaroni, R., 1999, *Langmuir, 15*, 3915.

Lecomte, P., Drapier, I., Dubois, P., Teyssie´, P., Je´roˆme, R., 1997, *Macromolecules, 30*, 7631.

Lee, D. C., Jang, L. W., 1996, Preparation and characterization of PMMA-clay hybrid composite by emulsion polymerization, *J. Appl. Polym. Sci.*, 61, 1117.

Lee, D.C., Jang, L.W., 1998, Characterization of epoxy-clay hybrid composite prepared by emulsion polymerization, *J. Appl. Polym. Sci.,* 68, 2005.

Lee, J., Giannelis, E., 1997, Polym. Prepr., 38, 688.

[a]**Matyjaszewski, K, Xia, j.,** 2001, *Chem. Rev., 101,* 2942, 2942, 2990.

REFERENCES (Continued)

[a.]**Matyjaszewski, K.,** 1998, *Macromol. Symp. , 134*, 105.

Matyjaszewski, K., 1999, *Chem. Eur. J., 5*, 3095.

[b.]**Matyjaszewski, K.; Beers, K. L.; Muhlebach, A.; Coca, S.; Zhang, X.; Gaynor, S. G.,** 1998, *Polym. Mater. Sci. Eng.*, *79*, 429-430.

[p1]**Matyjaszewski, K., Coca, S., Gaynor, S. G., Greszta, D., Patten, T. E., Wang, J.-s., Xia, J. WO** Pat. 9718247, U.S. Pat. 5,807,-937.

[p2]**Matyjaszewski, K., Coca, S., Gaynor, S. G., Nakagawa, Y., Jo, S. M. WO** Pat. 9801480, U.S. Pat. 5,789,487.

[a.]**Matyjaszewski, K., Coca, S., Gaynor, S. G., Wei, M., Woodworth, B., E.,** 1997, *Macromolecules , 30*, 7348.

[c.]**Matyjaszewski, K., Coca, S., Gaynor, S. G., Wei, M., Woodworth, B., E.,** 1998, *Macromolecules, 31*, 5967.

[b.]**Matyjaszewski, K.; Coca, S.; Jasieczek, C. B. *Macromol. Chem. Phys.,*** 1997, *198*, 4011-4017.

Matyjaszewski, K., Ed., 1996, *Cationic Polymerizations: Mechanisms, Synthesis and Applications*, Marcel Dekker: New York.

Matyjaszewski, K., Gaynor, S. G., Wang, J., S., 1995, *Macromolecules, 28*, 2093.

Matyjaszewski, K., Gaynor, S., G., 2000, In *Applied Polymer Science*, Craver, C. D., Carraher, C. E., Jr., Eds., Pergamon Press: Oxford, 929.

[b]**Matyjaszewski, K., Goebelt, B., Paik, H.-j., Horwitz, C., P.,** 2001, *Macromolecules, 34*, 430.

[c]**Matyjaszewski, K., Jo, S., M., Paik, H., j., Gaynor, S., G.,** 1997, *Macromolecules, 30*, 6398.

[c]**Matyjaszewski, K., Paik, H.-j., Zhou, P., Diamanti, S., J.,** 2001, *Macromolecules*, *34*, 5125.

[d]**Matyjaszewski, K., Patten, T., E., Xia, J.,** 1997, *J. Am. Chem. Soc., 119*, 674.

REFERENCES (Continued)

[d]Matyjaszewski, K., Shipp, D., A., Wang, J., L., Grimaud, T., Patten, T., E., 1998, *Macromolecules, 31*, 6836.

Matyjaszewski, K., Sigwalt, P., 1994, *Polym. Int., 35*, 1.

[e]Matyjaszewski, K., Wang, J., L., Grimaud, T., Shipp, D., A., 1998, *Macromolecules, 31*, 1527.

[p3]Matyjaszewski, K., Wang, J., S., WO Pat., 9630421, U.S. Pat. 5,-763, 548.

[f.]Matyjaszewski, K., Wei, M., Xia, J., Gaynor, S., G., 1998, *Macromol. Chem. Phys., 199*, 2289.

[e]Matyjaszewski, K., Wei, M., Xia, J., McDermott, N., E., 1997, *Macromolecules, 30*, 8161.

Menapace, R., Skorpik, C., Juchem, M., Scheidel, W., Schranz, R., 1989, Evaluation of the 1st 60 Cases of Poly Hema Posterior Chamber Lenses Implanted in the Sulcus., *Journal of Cataract and Refractive Surgery,* 15, (3), 264-271.

Messersmith, P. B., and Giannelis, E. P., 1994, Synthesis and characterisation of layered silicate-epoxy nanocomposites, *Chem. Mater*., **6**, 1719-1725.

Messersmith, P. B., and Giannelis, E. P., 1995, Synthesis and barrier properties of poly(ε-caprolactone)- layered silicate nanocomposites, *J. Appl. Polym. Sci. Part A*, **33**, 1047-1057.

Minisci, F., 1975, *Acc. Chem. Res., 8*, 165.

[a]Moineau, G., Dubois, P., Je´roˆme, R., Senninger, T., Teyssie´, P., 1998, *Macromolecules, 31*, 545.

[b]Moineau, G., Granel, C., Dubois, P., Je´roˆme, R., Teyssie´, P., 1998, *Macromolecules*, *31*, 542.

Moineau, G., Minet, M., Dubois, P., Teyssie´, P., Senninger, T., Je´roˆme, R., 1999, *Macromolecules*, *32*, 27.

REFERENCES (Continued)

Moineau, G., Minet, M., Teyssie´, P., Jerome, R., 2000, *Macromol. Chem., Phys, 201*, 1108.

Montheard, J. P., Chatzopoulos, M., Chappard, D., 1992, 2-Hydroxyethyl Methacrylate (Hema) - Chemical-Properties and Applications in Biomedical Fields., *Journal of Macromolecular Science-Reviews in Macromolecular Chemistry and Physics,* C32, (1), 1-34.

Nishikawa, T., Ando, T., Kamigaito, M., Sawamoto, M., 1997, *Macromolecules*, *30*, 2244.

Nishikawa, T., Kamigaito, M., Sawamoto, M., 1999, *Macromolecules*, *32*, 2204.

Nojiri, C., Okano, T., Koyanagi, H., Nakahama, S., Park, K., D., Kim, S., W., 1992, Invivo Protein Adsorption on Polymers - Visualization of Adsorbed Proteins on Vascular Implants in Dogs., *Journal of Biomaterials Science-Polymer Edition,* 4, (2), 75-88.

Ogata, N., Kawakage, S., Ogihara, T., 1997, Poly(vinyl alcohol)±clay and poly(ethylene oxide)-clay blend prepared using water as solvent, J. Appl. Polym. Sci., 66, 573-581.

Okada, A., Kawasumi, M., Usuki, A., Kojima, Y., Kurauchi, T., and Kamigaito O., 1990, Nylon 6-clay hybrid, *Mater. Res. Soc. Proc*., 171, 45-50.

Oriakhi, C., Nano sandwiches., 1998, Chem. Br., 34, 59.

Oriakhi, C.O., Farr, I.V., Lerner, M.M., 1997, Thermal characterization of poly(styrene sulfonate)/layered double hydroxide nanocomposites, Clays and Clay Minerals 45, 194.

Otsu, T., Tazaki, T., Yoshioka, M., 1990, *Chem. Express*, *5*, 801-802.

Ozawa, T., 1965, A new method of analysing thermogravimetric data, Bulletin of Chemical Society of Japan, 38, 881p.

Patten, T. E., Matyjaszewski, K., 1998, *Adv. Mater., 10*, 901.

Patten, T. E., Matyjaszewski, K., 1999, Acc. *Chem. Res., 32*, 895.

REFERENCES (Continued)

Percec, V., Barboiu, B., 1995, *Macromolecules*, *28*, 7970.

Percec, V., Barboiu, B., Bera, T. K., van der Sluis, M., Grubbs, R. B., Frechet, J. M. J., 2000, *J. Polym. Sci., Part A: Polym. Chem., 38*, 4776.

Percec, V., Barboiu, B., Kim, H. J., 1998, *J. Am. Chem. Soc., 120*, 305.

Percec, V., Barboiu, B., Neumann, A., Ronda., 1996, *Macromolecules, 29*, 3665.

Percec, V., Kim, H. J., Barboiu, B., 1997, *Macromolecules, 30*,8526.

Pittelkow, M., Lewinsky, R ., Christensen, J.B., 2002, Synthesis , 15, 2195.

Qiu, J., Matyjaszewski, K., 1997, *Acta Polym., 48*, 169.

Queffelec, J., Gaynor, S. G., Matyjaszewski, K., 2000, *Macromolecules, 33*, 8629.

[a]Ray, S. S., Okamoto, K, Okamoto, M., 2003, Structure–property relationship in biodegradable poly(butylene succinate)/layered silicate nanocomposites, *Macromolecules*, 36, 2355–67.

[b]Ray, S. S., Okamoto, M., 2003, *Prog. Polym. Sci.,* 28, 1542, 1545, 1546, 1607..

Ray, S. S., Yamada, K., Okamoto, M., Ueda, K., 2002, New polylactide/layered silicate nanocomposite: a novel biodegradable material., Nano Lett., 2, 1093–6.

Robbins, E. M., 2002, Ph.D Thesis, p:8.

Sefton, M. V., Nishimura, E., 1980, Insulin Permeability of Hydrophilic Polyacrylate Membranes., *Journal of Pharmaceutical Sciences,* 69, (2), 208-209.

Seki, T., Kawaguchi, T., Sugibayashi, K., Juni, K., Morimoto, Y., 1989, Percutaneous-Absorption of Azidothymidine in Rats. *International Journal of Pharmaceutics,* 57, (1), 73-75.

REFERENCES (Continued)

Shipp, D. A., Wang, J. L., Matyjaszewski, K., 1998, *Macromolecules,31*, 8005.

[a]**Simal, F., Demonceau, A., Noels, A., F.,** 1999, *Angew. Chem., Int. Ed. Engl., 38*, 538.

[b]**Simal, F., Demonceau, A., Noels, A., F.,** 1999, *Tetrahedron Lett., 40*, 5689.

Simal, F., Jan, D., Demonceau, A., Noels, A., F., 2000, *ACS Symp. Ser., 768*, 223.

Singha, N. K., Klumperman, B., 2000, *Macromol. Rapid Commun., 21*, 1116.

Takahashi, H., Ando, T., Kamigaito, M., Sawamoto, M., 1999, *Macromolecules, 32*, 3820.

Tatemoto, M., Oka, M., 1984, *Contemp. Topics Polym. Sci.,4*, 763.

Teodorescu, M.; Matyjaszewski, K., 2000, *Macromol. Rapid Commun.* 21, 190-194.

Terada, S., Suzuki, K., Nozaki, M., Okano, T., Takemura, N., 1997, Anti-thrombogenic effects of 2-hydroxyethylmethacrylate-styrene block copolymer and argatroban in synthetic small-caliber vascular grafts in a rabbit inferior vena cava model., *Journal of Reconstructive Microsurgery,* 13, (1), 9-16.

Tong, J. D., Moineau, G., Leclere, P., Bredas, J. L., Lazzaroni, R., Jerome, R., 2000, *Macromolecules, 33*, 470.

Uegaki, H., Kamigato, M., Sawamoto, M., 1999, *J. Polym. Sci., Part A: Polym. Chem.,37*, 3003.

Uegaki, H., Kotani, Y., Kamigato, M., Sawamoto, M., 1997, *Macromolecules, 30*, 2249.

Uegaki, H., Kotani, Y., Kamigato, M., Sawamoto, M., 1998, *Macromolecules*, *31*, 6756.

Vaia, R. A., Giannelis, E. P., 1997, Lattice of polymer melt intercalation

REFERENCES (Continued)

in organically-modified layered silicates., Macromolecules, 30, 7990–9.

Vaia, R. A., Price, G., Ruth, P. N., Nguyen, H. T., Lichtenhan, J., 1999, Polymer/layered silicate nanocomposites as high performance ablative materials., *Appl. Clay Sci*., 15, 67–92.

Vaia, R. A., Teukolsky, R. K., Giannelis, E. P., 1994, Interlayer structure and molecular environment of alkylammonium layered silicates, Chem. Mater., 6, 1017–22.

Wakioka, M., Baek, K. Y., Ando, T., Kamigaito, M., Sawamoto, M., 2002, *Macromolecules*, *35*, 330-333.

Wang, G., L., Hu, C. P., Ying, S. K., 1999, *Polymer, 40*, 2167.

Wang, J. L.; Grimaud, T.; Matyjaszewski, K., 1997, *Macromolecules*, *30*, 6507-6512.

[a]Wang, J. S., Matyjaszewski, K., 1995, *J. Am. Chem. Soc., 117*, 5614.

[b]Wang, J. S., Matyjaszewski, K., 1995, *Macromolecules, 28*, 7901, 7902.

Wang, Y., Herron, N., 1987, *J. Phys. Chem., 91*, 257.

Weimer, M. W., Chen, H., Giannelis, E. P., and Sogah, D. T., 1999, Direct synthesis of dispersed nanocomposites by in-situ living free radical polymerisation using a silicate-anchored initiator, *J. Am. Chem. Soc*., 121, 1615-1616.

Wichterle, O., Lim, D., 1960, Hydrophilic Gels for Biological Use.

Nature, 185, (4706), 117-118.

Wilson Jr., O., C., Olorunyolemi, T., Jaworski, Borum, A., L., Young, D., Siriwat, A., Dickens, E., Oriakhi, C., Lerner, M., 1999, Surface and interfacial properties of polymer-intercalated layered double hydroxide nanocomposites., *Appl. Clay Sci.,* 15, 265.

Wilson, M.J., 1987, A handbook of determinative methods in clay mineralogy, *Chapman and Hall*, New York..

REFERENCES (Continued)

Woodworth, B., E., Metzner, Z., Matyjaszewski, K., 1998, *Macromolecules, 31*, 7999.

Xia, J., Matyjaszewski, K., 1999, *Macromolecules*, *32*, 2434.

Xia, J., Zhang, X., Matyjaszewski, K., 2000, *ACS Symp. Ser., 760*, 207.

Xu, R., Manias, E., Snyder, A., J., Runt, J., 2001, New biomedical poly(urethane uera)-layered silicate nanocomposites, *Macromolecules*, 34, 337–9.

Yamaoka, K., Sasai, R., Takata, N., 2000, Colloids and Surfaces

A: Physicochemical and Engineering Aspects, 175, 23–39.

[a]**Yano, K., Usuki, A., Okada, A., Kurauchi, T., and Kamigaito, O.,** 1993, Synthesis and properties of polyimideclay hybrid, *J. Polym. Sci. Part A,* 31, 2493-2498.

[b]**Yano, K., Usuki, A., Okada, A., Kurauchi, T., Kamigaito, O.,** 1993, Synthesis and properties of polyimide–clay hybrid, *J. Polym. Sci*, Part A: Polym Chem., 31, 2491–93.

[a]**Zhao, H., and Shipp, D. A.,** 2003, *Chem. Mater*., 15, 2694

[b]**Zhao, H., Argoti, S. D., Farrel, B. P.,and Shipp, D. A.,** 2003, *J. Of Polymer Science: Part A, Ploymer Chemistry*, 42, 916.

Zanetti, M., Lomakin, S., Camino, G., 2000, Macromol Mater Eng. 279, 1.

CURRICULUM VITEA

Name Surname : Ayhan ORAL

Profession : Chemist

Date/ Place of Birth : 1972/Antalya

Nationnality : Turkish

Sex : Male

Martial Statue : Married

Adress : Ege University, Faculty of Science, Department of Chemistry, Division of Physical Chemistry, 35100 Bornova-Izmir/Turkey

E-mail : ayhan1oral@yahoo.com

EDUCATIONAL BACKGROUND

B.S. in Chemistry obtained in 1995, Inonu University, Malatya-Turkey

M.S. in Chemistry started in 2000, Canakkale Onsekiz Mart University, Canakkale-Turkey